J. Fluid Mech. (2001), *vol.* 440, *pp.* 205–234. Printed in the United Kingdom

The spreading of surfactant-laden liquids with surfactant transfer through the contact line

By ENRIQUE RAMÉ

The National Center for Microgravity Research on Fluids and Combustion,
NASA Glenn Research Center, 21000 Brookpark Road, MS 110-3, Cleveland, OH 44135, USA
e-mail: enrique.rame@grc.nasa.gov

(Received 31 August 2000 and in revised form 22 January 2001)

We examine the spreading of a liquid on a solid surface when the liquid surface has a spread monolayer of insoluble surfactant, and the surfactant transfers through the contact line between the liquid surface and the solid. We show that, as in surfactant-free systems, a singularity appears at the moving contact line. However, unlike surfactant-free systems, the singularity cannot be removed by the same assumptions as long as surfactant transfer takes place. In an attempt to avoid modelling difficulties posed by the question of how the singularity might be removed, we identify parameters which describe the dynamics of the macroscopic spreading process. These parameters, which depend on the details of the fluid motion next to the contact line as in the pure-fluid case, also depend on the state of the spread surfactant in the macroscopic region, in sharp contrast to the pure-fluid case where actions at the macroscopic scale did not affect material spreading parameters. A model of the viscous-controlled region near the contact line which accounts for surfactant transfer shows that, at steady state, some ranges of dynamic contact angles and of capillary number are forbidden. For a given surfactant–liquid pair, these disallowed ranges depend upon the actual contact angle and on the transfer flux of surfactant.

We also examine a possible inner model which accounts for the transfer via surface diffusivity and regularizes the stress via a slip model. We show that the asymptotic behaviour of this model at distances from the contact line large compared to the inner length scale matches to the viscous-controlled region. An example of how the information propagates is given.

1. Introduction

During the last 20 years many experimental and theoretical investigations have been devoted to the identification of predictive models for the spreading dynamics of single-component, isothermal fluids (Dussan V. 1979; de Gennes 1985; Kistler 1993). By contrast, the spreading of surfactant-laden liquids has received little attention by modellers. In this paper we address the spreading dynamics of an immiscible liquid–gas system advancing or receding on a solid in the presence of an insoluble surfactant. The spreading dynamics of surfactant-laden fluids differs from that of pure fluids in two ways. First, the surface tension is coupled to the flow through its dependence on surfactant concentration on the free surface. In addition, the surfactant can transfer from the interface onto the solid or vice versa. We will show that accounting for this transfer raises a non-trivial modelling issue. However, in spite of this difficulty, it is possible to identify parameters which describe the macroscopic dynamic interface

shape and the surface tension. In this section we review results for single-component systems, discuss how the presence of surfactants alters the physics of the displacement process, and conclude with modelling issues raised by the surfactant transfer.

1.1. *Pure liquids*

It is well known that when a Newtonian, incompressible fluid displaces another immiscible fluid across a rigid solid, a non-integrable stress appears at the moving contact line if the no-slip condition is enforced at the solid (Huh & Scriven 1971). From these assumptions (called collectively here 'the usual model' or 'the usual assumptions'), and without invoking linear momentum conservation, Dussan V. & Davis (1974) showed that a quantity, proportional to the force exerted by the fluid on the solid, must be unbounded. Consequently, this singularity cannot be removed by introducing any additional forces (e.g. van der Waals), and arises whenever the usual model is applied. The boundary value problem that results from this model is in fact ill-posed because the contact line singularity prevents one from using the contact angle as a boundary condition for the interface shape. This implies that new, unique mechanisms must replace the usual model very near the contact line. This idea led investigators to postulate the presence of an 'inner' region with length scale L_i, where these new mechanisms replace the usual assumptions, and an 'outer' or macroscopic region where the usual assumptions control the flow, scaled by the characteristic length of the flow, L_o. Since no suppositions have been made about the nature of the interface, these ideas apply to both pure and surfactant-laden fluids. Surprisingly, however, most of the work on contact line dynamics has focused on pure-fluid systems.

In the case of pure fluids, the 'inner' region next to the contact line has been examined both at the molecular and continuum levels. A number of molecular dynamics simulations have probed the nature of the boundary condition for a liquid in contact with a solid, under a variety of flow scenarios. Koplik, Banavar & Willemsen (1988), Thompson & Robbins (1990) and Hadjiconstantinou (1999) among others examined immiscible fluid displacement in simple flow geometries. Their results indicate that, in a two- to three-molecule distance from the contact line, the 'fluid' adjacent to the solid violates the no-slip condition. Newer molecular dynamics simulations by Thompson & Troian (1997) show that, given a fluid–solid pair, no-slip prevails at 'low' shear rates, $\dot{\gamma}$; slip $\sim \dot{\gamma}$ at moderate $\dot{\gamma}$; and, at higher shear rates slip becomes nonlinear in $\dot{\gamma}$. Finally, the ratio slip/$\dot{\gamma}$ diverges as $(\dot{\gamma} - \dot{\gamma}_c)^p$ $(p < 0)$ at a critical shear rate $\dot{\gamma}_c$. Continuum fluid mechanics analyses, on the other hand, cannot provide information about the nature of the boundary condition at the solid. Instead, they allow one to examine how the boundary value problem can be made well-posed by relaxing any of the usual assumptions. The most popular approach (adopted, for example by Hocking 1977; Dussan V. 1976; Huh & Mason 1977; Hocking & Rivers 1982; Sheng & Zhou 1992; and Finlow, Kota & Bose 1996 among many others) has been to relax the no-slip condition at the solid. However, allowing slip is by no means the only way of generating a well-posed boundary value problem. For example, Rosenblat & Davis (1985), Weidner & Schwartz (1994) and Voinov (1994) have assumed that the fluid becomes shear-thinning near the contact line.

The dynamic contact angle controls the spreading dynamics and the interface shape of pure fluids at low capillary number $Ca(\equiv U\mu/\sigma$, where U is the spreading velocity, μ the viscosity and σ the surface tension). In this regime, the inner-region parameters influence the dynamics through a single measurable parameter, ω_0, which depends on

L_i and the actual, inner contact angle, Θ_i, through

$$g_{pure}(\omega_0) = g_{pure}(\Theta_i) + Ca \ln(L_o/L_i), \tag{1.1}$$

where

$$g_{pure}(x) \equiv \int_0^x \frac{2 \sin u}{u - \sin u \cos u} \mathrm{d}u.$$

The identification and measurement of ω_0 has been the object of extensive analytical and experimental work by Hansen & Toong (1971), Kafka & Dussan V. (1979), Cox (1986*a*), Ngan & Dussan V. (1989), Dussan V., Ramé & Garoff (1991), Marsh, Garoff & Dussan V. (1993) and Chen, Ramé & Garoff (1995). As a result, the boundary condition for the macroscopic interface shape near the moving contact line of a pure fluid can be formulated as

$$\theta \sim g_{pure}^{-1}(g_{pure}(\omega_0) + Ca \ln(r/L_o)) + f_0(r/L_o; \omega_0) - \omega_0 \quad \text{as} \quad r/L_o \to 0. \tag{1.2}$$

Here, $g_{pure}^{-1}(g_{pure}(x)) = x$, θ is the slope of the interface relative to the solid, r is the distance from the contact line to a point on the interface, and f_0 denotes a static interface shape with contact angle ω_0 (refer to figure 1). Since ω_0 may be found at each Ca by fitting equation (1.2) to an experimentally measured interface shape very near the contact line, this approach does not necessitate knowledge of the physics in the inner region (see Chen *et al.* 1995).

1.2. *Surfactants*

Surfactants, which preferentially reside on the interface rather than in the bulk phases, affect both static (Adamson 1967) and dynamic wetting (Cox 1986*b*; Joanny 1989; Chesters & Elyousfi 1998). One of their more obvious effects is that they change the surface tension and the contact angle; however, these effects do not introduce any fundamental modelling difficulty besides perhaps the increased complexity of the analysis. The process that does introduce a non-trivial modelling difficulty is the transfer of surfactant from (to) the liquid surface to (from) the solid, found, for example, in Langmuir–Blodgett depositions but absent in the spreading of pure liquids. As expected, a stress singularity, similar to that in the pure-fluid case, reappears. However, this time the singularity cannot be removed by the same means as in pure fluids. Below we review the literature on spreading of surfactant-laden systems and discuss the additional modelling complications that arise when surfactants are present.

Spread monolayers of insoluble surfactants attracted the attention of surface chemists as a way to alter the outermost atomic layer of a solid, and hence change its surface properties. Langmuir (1920) and Blodgett (1935) found that a monomolecular layer of an insoluble surfactant (a fatty acid) spread on the surface of a liquid can transfer to a glass slide that is repeatedly immersed and withdrawn into and from the liquid. Behaviours during immersion and withdrawal may be vastly different. Langmuir (1920) and Blodgett (1935) observed moving contact lines during immersion; and Langmuir (1938) documented the presence of contact lines during withdrawal. However, Petrov, Kuhn & Möbius (1980) and Petrov (1986) found that there is a maximum speed of withdrawal, characteristic of each system, above which the contact line remains pinned to the solid. When this happens, instead of a moving contact line, a thin film of entrained liquid forms between the solid and the surfactant monolayer. This behaviour also appears in surfactant-free systems, but the fates of the respective entrained fluid layers differ (see e.g. Petrov & Sedev 1985; Sedev & Petrov 1991). In this paper we focus on situations where a well-defined contact line exists and surfactant transfers between the interface and the solid. Thus, we address advancing and

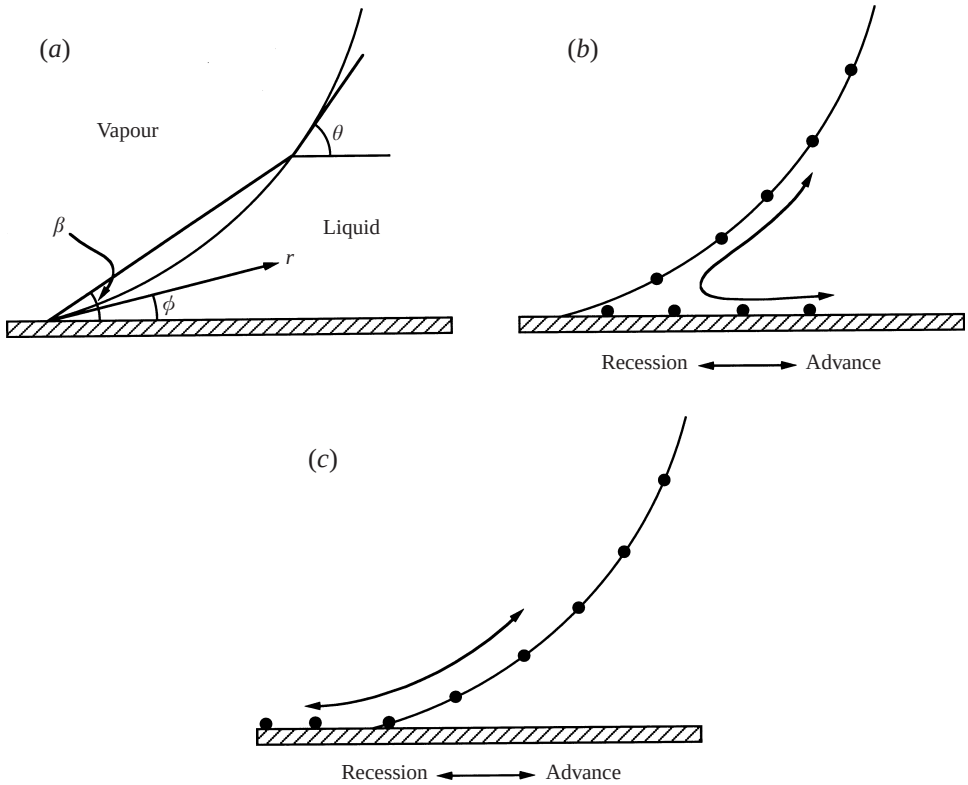

FIGURE 1. (*a*) Coordinate system used in the analysis of the intermediate region. Depending on the molecular interactions of the surfactant with the solid, liquid and vapour: (*b*) surfactant spread on the interface is deposited onto the solid–liquid surface during advance, and surfactant adsorbed on the solid–liquid surface may return to the interface during recession; (*c*) surfactant spread on the interface is deposited onto the solid–vapour surface during recession, and surfactant adsorbed on the solid–vapour surface may return to the interface during advance. Filled circles represent surfactant molecules.

receding motions far from the entrainment limit, with surfactants which are reactive enough to stick to the solid 'instantaneously' on the time scale of the flow, and which transfer from (onto) the interface onto (from) the solid; refer to figure 1.

Damania & Bose (1986) studied experimentally the effect of surfactant solutions on the spreading behaviour of liquids. They looked at shapes of dynamic menisci in a moving vertical flat plate for both pure fluids and surfactant systems. They showed that, when $Ca < 10^{-4}$, pure liquids form dynamic menisci whose shape is described well by the static theory. Under these conditions, the force exerted on the plate after correcting for buoyancy comes only from surface tension. This indicates that, at least in the region examined, viscous forces do not affect the shape of the interface nor do they exert a measurable drag on the plate. However, when surfactants are present, the force does not correspond to that of surface tension at the equilibrium surfactant concentration, and static theory cannot describe the shape, even at the small values of Ca where this was true in their surfactant-free systems. They also observed transient forces and meniscus shapes both with and without spreading. They interpreted these observations in terms of the relative transport of surfactant into the contact line via diffusion–convection, and away from it by adsorption on the

solid surface. Thus, soluble surfactants may transfer to the solid via dissolution in the bulk and readsorption to the solid from solution. It may be then possible for an 'almost insoluble' surfactant to transfer to the solid within a very small region near the contact line where solubility becomes important (see § 1.3).

At the continuum theory level, Cox (1986*b*) addressed the fluid mechanics of a spreading liquid with an insoluble surfactant in the special case where surfactant does not transfer onto the solid. His main objective was to establish how material information propagates from the inner to the outer region to form the macroscopic contact-angle boundary condition. Cox recognized that, when surfactants are present, a singularity appears at the contact line just as in the pure fluid case, but did not address the removal of the singularity. Instead, he assumed that it had been removed by some suitable inner mechanism such as slip. Perhaps coincidentally, a slip condition alone is sufficient to describe an adequate inner region in the zero-transfer case examined by Cox but not in the more general case with surfactant transfer. In fact, slip removes the singularity by making the fluid velocity relative to the contact line equal zero at the contact line. This fact prevents convective transfer of surfactant through the contact line which leads to the apparent contradiction, discussed in § 1.3, that if slip removes the singularity, surfactant cannot transfer by convection alone at the contact line.

Joanny (1989) examined the dynamics of spreading during deposition of a Langmuir–Blodgett film. In his formulation the chemical potentials of the surfactant are known in terms of the surfactant concentration on the solid and on the interface. This knowledge would allow one to compute the flux of surfactant mapped onto the solid. Using the lubrication approximation, Joanny focuses on the structure of the precursor film that precedes the spreading of the bulk liquid in systems where long-range (van der Waals) forces are important, and derives power laws for the velocity dependence of an apparent contact angle. Though Joanny recognizes that a force singularity still arises at the tip of the precursor film (see § 1.3), his assertion that van der Waals forces resolve the singularity by making the film intersect the solid at 90° at the tip is not at all obvious. In fact, Dussan V. & Davis (1974) have shown in a general way that, regardless of the nature of the forces acting on the fluid, the drag of a Newtonian liquid on the solid diverges at the contact line. Joanny, finally, addresses systems in which the surfactant concentration deposited on the solid is smaller than the concentration on the interface next to the solid (that is, the transfer ratio < 1). This limitation is imposed by the lubrication approximation. In our study, a transfer ratio of 1 is not special from a modelling standpoint as the transfer ratio merely provides an initial value for the interface velocity.

Troian, Herbolzheimer & Safran (1990) showed that when a droplet of a surfactant solution spreads on a thin layer of pure solvent, a Marangoni-driven instability develops at the edge of the drop which is mathematically similar to that arising in immiscible fluid displacement in a Hele-Shaw cell. Chesters & Elyousfi (1998) analysed the advancing motion of a surfactant-laden meniscus in a capillary tube with surfactant transfer onto the solid. The model exhibits interesting dynamics. In particular, a given distribution of surfactant concentration on the meniscus may coexist with multiple macroscopic contact angles depending on the time history of the meniscus concentration.

1.3. *The singularity in surfactant-laden systems*

Spread insoluble surfactants show a rich variety of behaviour. Depending on the materials, the surfactant may remain on the interface without being mapped onto the

solid (i.e. the interface is immobile as in Cox 1986*b*) or it may transfer to the solid at varying rates. The transfer may occur during the liquid-advancing cycle only, or during the liquid-receding cycle only, or during both (refer to figure 1). In any case, the interface is endowed with a surface velocity controlled primarily by the relative affinities of the solid and the interface for the surfactant molecules. In the remainder of this section we examine the modelling difficulty associated with the fluid motion in the vicinity of a moving contact line when the surfactant transfers through the contact line, and consider ways of generating a well-posed boundary value problem.

Consider an immiscible gas–liquid pair in contact with a planar solid surface. In a reference frame fixed at the moving contact line, the solid velocity U is constant and parallel to its surface. Without loss of generality, we assume: (*a*) the gas has negligible viscosity, so we ignore its motion; (*b*) the liquid does not diffuse through the gas nor does it adsorb onto the dry solid so that a hydrodynamic liquid layer does not exist ahead of the spreading body; and (*c*) the motion is steady and two-dimensional. For unsteady motions, the flow in a small region near the contact line of characteristic length R may be treated as quasi-steady as long as the time scale of the unsteadiness is large compared with the time scale for flow in the region under consideration, R/U (Cox 1986*a*, *b*).

In the absence of surface diffusion, the local mass flux of surfactant on the interface is $\Gamma \boldsymbol{u}_\Gamma$, where $\boldsymbol{u}_\Gamma$ is the mass-averaged velocity on the interface and Γ is the surface concentration. In the frame of reference fixed at the contact line, $\boldsymbol{u}_\Gamma$ is wholly tangent to the interface. When surfactant transfers directly onto the solid, $\Gamma \boldsymbol{u}_\Gamma \neq 0$ at the contact line. Since Γ is bounded, $\boldsymbol{u}_\Gamma$ must be tangent to the interface and $\neq 0$ at the contact line. On the other hand, the velocity of fluid points adjacent to the solid must be wholly tangent to the solid. Therefore, the velocity field must be multivalued at the contact line as long as surfactant transfers directly by convection through the contact line. Since all known slip models regularize the stress by making the velocity at the contact line $\boldsymbol{u}_{CL} = \boldsymbol{0}$, slip would prevent the transfer. This leads to the contradiction that, if slip removes the singularity, then convective surfactant transfer cannot take place. In order to resolve this contradiction, some other inner mechanism(s) must be present besides slip which can account for the transfer and be consistent with slip.

Examples of inner mechanisms that could account for surfactant transfer include surface diffusion and modelling the surfactant as 'almost insoluble'. Alternatively, one might postulate the existence of a 'surface phase' of finite – albeit very small – thickness, to which the surfactant is confined. This phase would most likely be anisotropic, having a constitutive nature different from that of the fluid; therefore, an infinite force need not arise. Both surface diffusion and finite-thickness surface phase could amount to *effective slip* at the interface. None of these alternatives has yet been thoroughly explored, though Ramé (1988) briefly discussed models applied to surfactant systems and Shikhmurzaev (1993, 1997) has developed extensively surface-phase models for pure fluids.

Inner models affect the details of the flow only on a very small inner length scale L_i about the contact line.† Regardless of these details, inner-region parameters have a significant impact on the macroscopic behaviour of a spreading fluid only through the dynamic contact angle when $Ca \ll 1$. For pure fluids, equation (1.2) shows that, when $Ca \ll 1$, the interface shape near the contact line can be expressed

† L_i is small compared to the macroscopic scale but must be large enough for continuum theory to apply. Previous analyses for pure fluids have assumed thate L_i is of molecular dimension, i.e. between 10 Å and 1000 Å (see e.g. Hocking & Rivers 1982 and Cox 1986*a*).

as $\theta \sim F_1(C + Ca\ln r) + F_2(C + Ca\ln(L_o), r/L_o)$. The material constant C, depends on inner-region parameters through $C = g_{pure}(\Theta_i) - Ca\ln(L_i)$. This form has been shown to be independent of the inner model for a wide range of slip boundary conditions. Consequently, it is C and not the particular inner model that controls the macroscopic interface shape through the parameter $\omega_0 = g^{-1}_{pure}(g_{pure}(C + Ca\ln L_o))$, where ω_0 is defined in equation (1.2).

Since C (or ω_0) can be determined experimentally by macroscopic measurements, it is thus possible, when $Ca \ll 1$, to parameterize the macroscopic flow without addressing the flow in the inner region. This fact is crucial because discovering inner mechanisms does not seem likely at the present time. On the one hand, due to its extremely small length scale, there have not been direct probings of the inner region which successfully shed light on the physics of the displacement process there. On the other hand, the dependence of C on inner parameters through a single expression independent of the inner model suggests that it is impossible to look into the physics of the inner region using macroscopic measurements of C. Nevertheless, it is possible to parameterize macroscopic spreading dynamics. Experiments on the spreading of pure fluids showed the presence of a region, approximately located at $10\,\mu m < r < 300\,\mu m$ from the contact line, where the interface slope, θ, is a dynamic material property independent of the macroscopic geometry and given by equation (1.2). This portion of the interface shape contains material information which describes the dynamics of the macroscopic spreading process (Dussan V. *et al.* 1991). Motivated by this approach, and since for most practical applications the dynamics of the outer region are of primary interest, we will seek a macroscopic parametrization of the spreading dynamics of surfactant-laden systems which does not rely on knowledge of inner models.

Specifically, we seek the apparent or macroscopic dynamic contact angle in terms of a suitably defined Ca, constants characterizing the interface shape and surface tension, transfer rate of surfactant, and the surfactant equation of state. In the next section we address the model and problem formulation. We will show that the surfactant management strategy in the macroscopic region does affect the dynamics of the interface (and thus the dynamic contact angle) in the viscous region near the moving contact line. By matching to a macroscopic region in the small-Ca limit, in § 3 we identify the apparent contact angle for the macroscopic interface shape. Matching to the inner region yields a complete set of conditions to integrate the equations governing the interface shape and surfactant concentration. We then examine the dynamic behaviour of the apparent contact angle for various transfer rates of surfactant at steady macroscopic concentrations, and derive approximate closed-form expressions for the contact angle in terms of properties defined in the inner region. We conclude by discussing in § 4 a possible inner model, developed within the lubrication approximation, which accounts for surfactant transfer via surface diffusivity. This model may be used to examine how surface tension and interface velocity information is transmitted outwards to the viscous, non-diffusing region.

2. Formulation and solution

We are interested in the case when surface tension and viscous forces balance at lowest order near the contact line under conditions of $Ca \ll 1$ and $\varepsilon \equiv L_i/L_o \ll 1$. To capture this balance we must have $\eta \equiv -Ca\ln(\varepsilon) = O(1)$ as $Ca \to 0$. In this limit the inner and outer regions are connected by an intermediate region where significant

viscous effects are present. Here we follow the method developed by Hocking & Rivers (1982) and Cox (1986*a*, *b*) for analysing the intermediate region.

It is assumed that some suitable mechanism has removed the stress singularity in the inner region. Though the exact nature of this mechanism is not important for now, the interface shape must behave like

$$\theta \sim \Theta_i + Ca\{H(\Theta_i)\ln(r/L_i) + l_i(\Theta_i)\}, \quad \Theta_i \neq 0, \tag{2.1a}$$

$$\theta \sim (A\,Ca\ln(r/L_i))^{1/3}, \quad \Theta_i = 0, \tag{2.1b}$$

as $r/L_i \to \infty$ independently of the inner mechanism. Here Θ_i is the actual contact angle found at the scale of the inner region, $l_i(\Theta_i)$ and A depend on the inner physics, $H(\theta)$ is known and independent of the inner model, and r is the (dimensional) distance from the contact line to a point on the free surface. In general, Θ_i may depend on the dimensional spreading velocity, U, and surfactant concentration next to the contact line, Γ_{CL}. The outer region lies far from the contact line. As $r/L_o \to 0$ in the outer region, the interface shape behaves as

$$\theta \sim \omega_0 + Ca\{H(\omega_0)\ln(r/L_o) + l_o(\omega_0)\}, \tag{2.2}$$

where ω_0 (defined in equation (1.2)) and $l_o(\omega_0)$ must be determined by matching.

Our analysis focuses on the intermediate region of expansion where the flow obeys the usual hydrodynamic model and is not influenced by the macroscopic geometry. We define the following scales: $\boldsymbol{u} \sim |U|, r \sim L_o, p \sim \sigma^*/L_o, \sigma \sim \sigma^*, \Gamma \sim \Gamma^*$. Here U is the velocity of the contact line relative to the solid and $U > 0$ denotes advancing motion; Γ^* and σ^* will be identified below. In what follows, the variables $\boldsymbol{u}$, p, r, σ and Γ must be considered dimensionless unless otherwise noted.

The geometry of the intermediate region resembles a wedge with a slowly varying aperture; refer to figure 1. The choice of independent variable, $\xi \equiv Ca\ln(r)$, ensures that the dependent variables vary slowly with r. Further, $-\eta < \xi < 0$ and $r = \exp(\xi/Ca)$, so that, for ξ fixed with $Ca \ll 1$, it follows that $\varepsilon \ll r \ll 1$ exponentially in Ca. Next we identify the scales σ^* and Γ^*.

2.1. *Scales for σ and Γ*

Since Γ and σ are related through the equation of state for the spread monolayer, it is only necessary to identify the scale Γ^*. Without loss of generality, we examine the following thought experiment. An operator controls the concentration of a spread surfactant monolayer in the outer (or macroscopic) region by means of a barrier deployed on the interface. By moving the barrier, the operator can affect the concentration not only in the outer but also in the inner and intermediate regions. Since the dynamic contact angle Θ_i may depend on the surfactant concentration at the contact line, it follows that, in systems with surfactants, a mechanism exists for information to be passed from the outer back to the intermediate and inner regions. This is a remarkable departure from pure-fluid systems where Θ_i is typically assumed to be strictly a consequence of the local dynamics near the moving contact line (Ngan & Dussan V. 1989) and cannot be affected by actions in the outer region.

Despite this inner–outer feedback loop, the concentration in the outer region decouples from that in the intermediate and inner regions to lowest order as $Ca \to 0$. This is because the inner and intermediate regions are exponentially small as $Ca \to 0$ and the surface concentration is bounded. Consequently, it is possible to control the

surfactant concentration in the outer region independently of the mass inventory in the inner and intermediate regions. We therefore consider only the mass in the outer region. Because viscous effects are zero to lowest order as $Ca \to 0$ in the outer region, surface tension and concentration are independent of position at this order. Under these conditions, and neglecting surface diffusion of surfactant adsorbed on the solid, mass conservation for the surfactant in the outer region, valid at $O(1)$ as $Ca \to 0$ requires

$$M_{ini} - \Gamma_s U t = \Gamma(t) L(t), \tag{2.3}$$

where all variables are dimensional, M_{ini} is the initial mass on the interface per unit length of the contact line, Γ_s is the surfactant concentration on the solid as it passes the contact line, t is time, L is the interface length covered with surfactant and $\Gamma_s U$ is the (convective) flux of surfactant carried by the solid. Using the scales, $L \to L_o$,† $t \to L_o/U$, and choosing $\Gamma^* \equiv M_{ini}/(L_o L_{ini})$, with L_{ini} the dimensionless initial interface length, equation (2.3) is non-dimensionalized:

$$L_{ini} - \Gamma_s t = \Gamma(t) L(t). \tag{2.4}$$

Γ_s is known as the 'transfer ratio' in the Langmuir–Blodgett literature.

During a typical monolayer transfer, the surface concentration may be held constant by a suitable motion of the barrier used to confine the spread monolayer. Alternatively, the barrier position may be held fixed so that the surface tension increases/decreases in time as transfer of surfactant to/from the solid lowers/raises the surface concentration. At leading order as $Ca \to 0$, the laws governing the barrier motion needed to hold the surface tension constant and the time rate of change of the surface tension when the barrier is held fixed can be derived from equation (2.4). From the scaling just defined, it follows that $\Gamma = 1$ at $t = 0$. When the outer surface tension is held fixed, the barrier motion that keeps $\Gamma(t) = 1$ for $t > 0$ is $L(t) = L_{ini} - \Gamma_s t$. When the monolayer length L is fixed, the barrier does not move but Γ changes with time according to $\Gamma(t) = 1 - \Gamma_s t/L_{ini}$. These examples of control protocols in the outer region set up the matching condition for the surface tension in the intermediate region (see equations (3.4) and (3.5)).

2.2. *Governing equations and boundary conditions*

We use polar coordinates (r, ϕ) centred at the contact line. The interface location is $\phi = \beta(r)$ and the solid (assumed flat) is at $\phi = 0$; refer to figure 1. The governing equations are the conservation of linear momentum and mass for a Newtonian, incompressible fluid, subject to the usual boundary conditions of continuity of velocity at solid boundaries and continuity of stress, velocity and surfactant mass at the free surface. With the scalings defined above, the dimensionless parameters are $We = \rho U^2 L_o/\sigma^*$, $Bd = \rho g L_o^2/\sigma^*$ and $Ca = U\mu/\sigma^*$. Since $r \ll 1$, we may neglect gravity and inertia, and assume the flow to be planar and two-dimensional. We may then define a stream function which satisfies the biharmonic equation and may be written as $\psi = rg(\phi, \xi)$. The dependence of g on ξ captures the slow variation with r introduced by the non-constant interface angle. The velocity components are then

$$u = \partial g/\partial \phi, \quad v = -(g + Ca\, \partial g/\partial \xi).$$

Expressions for the pressure, stress, and normal and tangential velocities can also be derived, and boundary conditions may be written for $g(\phi, \xi)$ (Cox 1986*b*).

† If a solid plate is immersed in a large liquid bath on Earth, L_o is the capillary length $(\sigma/\rho g)^{1/2}$ where g is the acceleration due to gravity.

Surface tension depends on surface concentration through an equation of state. When this equation is linearized about and made dimensionless by (σ^*, Γ^*), it is

$$\sigma - 1 = \gamma(\Gamma - 1), \tag{2.5}$$

where $\gamma \equiv (\mathrm{d}\sigma/\mathrm{d}\Gamma)^*(\Gamma^*/\sigma^*)$. Since surfactant can transfer through the contact line, we need to allow for a non-zero surfactant flux at the interface. As discussed in § 1.3, convective transfer at the contact line gives rise to a singularity that cannot be removed if surfactant transfers only by convection. (In § 4 we illustrate how surface diffusivity can be used to generate a well-posed problem.) However, transport in the intermediate region is mainly convective provided the surface Péclet number $UL_o/D_s \gg 1$, D_s being the surface diffusivity. If we assume steady state,† the mass flux on the interface must equal the surfactant flux carried by the solid, i.e. the solid takes away (supplies) all the surfactant leaving (entering) the free surface. Thus, conservation of surfactant mass requires that

$$\Gamma_s = -\Gamma u_\tau = \text{constant}, \tag{2.6}$$

where Γ_s is defined in equation (2.3), and $u_\tau = \boldsymbol{u} \cdot \boldsymbol{\tau}$ is the velocity component tangent to the interface with the unit tangent vector $\boldsymbol{\tau}$ pointing away from the contact line. In our convention $\Gamma_s > 0$ corresponds to surfactant being deposited onto the solid, i.e. $u_\tau < 0$. If surfactant were to leave the solid and return to the interface, then $u_\tau > 0$ and $\Gamma_s < 0$ (see figure 1*b*, *c*). Equation (2.6) evaluated at the edge of the inner region is a mass balance around the contact line with the inner region excised. In this model, all the surfactant entering the inner region on the free surface is taken away convectively by the solid (see e.g. Chesters & Elyousfi 1998). To complete the problem, the integral balance for the surfactant mass is

$$L_{ini} - \Gamma_s t = \int_0^{L(t)} \Gamma(s, t)\, \mathrm{d}s. \tag{2.7}$$

We now state the leading-order boundary value problem as $Ca \to 0$ as in Cox (1986*b*).

2.3. *Lowest-order problem*

It is assumed that, in the limit $Ca \to 0$ with $Ca \ln(\varepsilon) = O(1)$, the generic independent variable, V, has an asymptotic expansion:

$$V(\phi, \xi; Ca, \Gamma_s) \sim V_0(\phi, \xi; \Gamma_s) + O(Ca).$$

In what follows we will omit the subscript 0 with the understanding that all the variables are the leading terms of this asymptotic expansion. The governing equation for $g(\phi, \xi)$ is

$$\left(\frac{\partial^2}{\partial \phi^2} + 1\right)^2 g = 0. \tag{2.8a}$$

The kinematic boundary condition at the solid reduces to

$$g = 0, \quad \frac{\partial g}{\partial \phi} = \pm 1 \quad \text{on} \quad \phi = 0, \tag{2.8b, c}$$

with the plus and minus signs denoting advancing and receding liquid, respectively. The kinematic condition, and normal and tangential stress balances on the free surface

† Even if the outer region is not in steady state it is possible, since $L_i \ll L_o$, for the inner region to look quasi-steady so that equation (2.6) will hold (see Cox 1986*a*, *b*).

are, respectively:

$$g = 0, \quad \frac{\mathrm{d}\beta}{\mathrm{d}\xi} = \frac{1}{\sigma}\left[\frac{\partial g}{\partial \phi} + \frac{\partial^3 g}{\partial \phi^3}\right], \quad \frac{\mathrm{d}\sigma}{\mathrm{d}\xi} = \frac{\partial^2 g}{\partial \phi^2}$$

$$\text{(all evaluated at } \phi = \beta(\xi).) \tag{2.8d, e, f}$$

Finally, surfactant mass conservation, equation (2.6), requires

$$\partial g/\partial \phi = u_\tau (= -\Gamma_s/\Gamma) \quad \text{on} \quad \phi = \beta(\xi). \tag{2.8g}$$

When $\Gamma_s = 0$, surfactant does not transfer and we recover the problem analysed by Cox (1986*b*). The function $g(\phi, \xi)$ results from the solution to equation (2.8*a*) with boundary conditions (2.8*b–d*, *g*) The surface tension and concentration are related through the equation of state (2.5). The interface shape and surface tension result from integrating (2.8*e*, *f*) with appropriate boundary conditions to be derived by matching in § 3.

2.4. *Solution*

Even though the whole problem is nonlinear, the equations governing $g(\phi, \xi)$ form a linear problem driven by the unit velocity of the solid at $\phi = 0$, and by the tangential velocity of the free surface, $u_\tau (= -\Gamma_s/\Gamma)$. Although u_τ is a function of ξ, this variable acts as a parameter because $\partial^n g/\partial \xi^n$ does not appear in the boundary value problem (2.8*a–d*, *g*). It is therefore possible to decompose g as

$$g = g_1 + u_\tau g_2, \tag{2.9}$$

where g_1 and g_2 satisfy the same governing equation and boundary conditions as g, except that $\partial g_1/\partial \phi = 0$ on $\phi = \beta(\xi)$; and $\partial g_2/\partial \phi = 1$ on $\phi = \beta(\xi)$, $\partial g_2/\partial \phi = 0$ on $\phi = 0$. The function g_1 corresponds to the no-transfer case:

$$g_1 = \pm \frac{\phi \sin\beta \sin(\phi - \beta) + \beta(\beta - \phi)\sin\phi}{\beta^2 - \sin^2\beta} \tag{2.10a}$$

and

$$g_2 = \frac{\beta \sin\beta(\sin\phi - \phi\cos\phi) - \phi\sin\phi(\sin\beta - \beta\cos\beta)}{\beta^2 - \sin^2\beta}. \tag{2.10b}$$

In order to obtain the interface shape, $\beta(\xi)$, and the surface tension, $\sigma(\xi)$, we must solve the coupled equations (2.8*e*, *f*). For consistency with (2.9), we rewrite these equations as

$$\frac{\mathrm{d}\beta}{\mathrm{d}\xi} = \frac{1}{\sigma}(f_1(\beta) + u_\tau f_2(\beta)), \quad \frac{\mathrm{d}\sigma}{\mathrm{d}\xi} = h_1(\beta) + u_\tau h_2(\beta), \tag{2.11a, b}$$

where

$$f_1(\beta) = \frac{\partial g_1}{\partial \phi} + \frac{\partial^3 g_1}{\partial \phi^3}\bigg|_{\phi=\beta} = \frac{\pm 2\beta \sin\beta}{\beta^2 - \sin^2\beta}, \quad f_2(\beta) = \frac{\partial g_2}{\partial \phi} + \frac{\partial^3 g_2}{\partial \phi^3}\bigg|_{\phi=\beta} = \frac{2\sin^2\beta}{\beta^2 - \sin^2\beta}.$$

$$h_1(\beta) = \frac{\partial^2 g_1}{\partial \phi^2}\bigg|_{\phi=\beta} = \pm 2\frac{\sin\beta - \beta\cos\beta}{\beta^2 - \sin^2\beta}, \quad h_2(\beta) = \frac{\partial^2 g_2}{\partial \phi^2}\bigg|_{\phi=\beta} = \frac{2\beta - \sin 2\beta}{\beta^2 - \sin^2\beta},$$

Since $u_\tau = -\Gamma_s/\Gamma$ and $\Gamma = 1 + (1 - \sigma)/\gamma$, equations (2.11) cannot be integrated in closed form. Boundary conditions for numerical integration will be derived by matching to the outer and the inner regions.

2.5. *Limit of small transfer ratio, $\Gamma_s \ll 1$*

In order to study analytically the influence of surfactant transfer rate on the surface tension and interface shape, we expand the zeroth order of the Ca-expansion in powers of Γ_s, valid for $\Gamma_s \to 0$:

$$\sigma \sim \sigma_0 + \Gamma_s \sigma_1 + \cdots,$$

with analogous expressions for Γ and β. Substitution in equation (2.11) generates problems at $O(1)$ and $O(\Gamma_s)$. In this limit, σ and β decouple at lowest order:
$O(1)$:

$$\frac{\mathrm{d}\sigma_0}{\mathrm{d}\xi} = h_1(\beta_0), \quad \frac{\mathrm{d}\beta_0}{\mathrm{d}\xi} = \frac{1}{\sigma_0} f_1(\beta_0). \tag{2.12a,b}$$

If we divide (2.12a) by (2.12b), the resulting equation can be integrated exactly:

$$\sigma_0 = K_{\sigma 0} \frac{\beta_0}{\sin \beta_0}, \quad \Gamma_0 = 1 + (\sigma_0 - 1)/\gamma, \tag{2.13a,b}$$

where $K_{\sigma 0}$ is an integration constant. The interface shape is given implicitly by the integral of equation (2.12b), which, after substitution of the solution for σ_0, becomes

$$\xi + K_{\theta 0} = K_{\sigma 0} G_0(\beta_0), \tag{2.14}$$

where

$$G_0(\beta_0) \equiv \pm \int_0^{\beta_0} \frac{\beta^2 - \sin^2 \beta}{2 \sin^2 \beta} \mathrm{d}\beta, \tag{2.15}$$

and $K_{\theta 0}$ is another integration constant. These results follow from Cox (1986b) when the viscosity of the displaced phase is zero ($\lambda = 0$ in Cox's notation).
$O(\Gamma_s)$:

$$\frac{\mathrm{d}\beta_1}{\mathrm{d}\xi} = -\frac{1}{\sigma_0} \frac{f_2(\beta_0)}{\Gamma_0} - \frac{\sigma_1}{\sigma_0^2} f_1(\beta_0) + \frac{1}{\sigma_0} \frac{\mathrm{d}f_1}{\mathrm{d}\beta}\bigg|_{\beta_0} \beta_1 \tag{2.16a}$$

$$\frac{\mathrm{d}\sigma_1}{\mathrm{d}\xi} = -\frac{h_2(\beta_0)}{\Gamma_0} + \frac{\mathrm{d}h_1}{\mathrm{d}\beta}\bigg|_{\beta_0} \beta_1. \tag{2.16b}$$

It is simpler to continue using β_0 as the independent variable, so we divide through by equation (2.12b):

$$\frac{\mathrm{d}\beta_1}{\mathrm{d}\beta_0} = -\frac{1}{\Gamma_0} \frac{f_2(\beta_0)}{f_1(\beta_0)} - \frac{\sigma_1}{\sigma_0} + \frac{\beta_1}{f_1(\beta_0)} \frac{\mathrm{d}f_1}{\mathrm{d}\beta}\bigg|_{\beta_0} \tag{2.17a}$$

$$\frac{\mathrm{d}\sigma_1}{\mathrm{d}\beta_0} = \frac{\sigma_0}{f_1(\beta_0)} \left[-\frac{h_2(\beta_0)}{\Gamma_0} + \frac{\mathrm{d}h_1}{\mathrm{d}\beta}\bigg|_{\beta_0} \beta_1 \right]. \tag{2.17b}$$

These coupled ordinary differential equations are not solvable in closed form. However, a two-term series solution valid for $\beta_0 \ll 1$ gives reasonable quantitative and good qualitative agreement in the whole range of β_0 for the small Γ_s tested. It is easily shown that

$$\sigma_1 \sim \pm 5 \frac{K_{\sigma 0}}{K_{\Gamma_0}} + K_{\sigma 1} \left[1 + \frac{\beta_0^2}{18} \right] \quad \text{as} \quad \beta_0 \to 0, \tag{2.18a}$$

$$\beta_1 \sim -\beta_0 \left(\pm \frac{2}{K_{\Gamma 0}} + \frac{K_{\sigma 1}}{3 K_{\sigma 0}} \right) \quad \text{as} \quad \beta_0 \to 0, \tag{2.18b}$$

where $K_{\sigma 1}$ is a constant and $K_{\Gamma 0} \equiv 1+(K_{\sigma 0}-1)/\gamma$. Boundary conditions for equations (2.11a, b) and the values of $K_{\theta 0}, K_{\sigma 0}, K_{\sigma 1}$ will be found below by matching.

3. Results and discussion

Our results fall into two categories, which may be loosely termed 'modelling' and 'dynamic behaviour'. First, in the modelling category, we derive boundary conditions for equations (2.11) by matching the intermediate region solution to the solutions in the outer and inner regions. To address the most general case possible, we first perform the match for arbitrary transfer flux, Γ_s. Since this case only admits numerical solutions, it cannot be used to extract the dependence of the macroscopic contact angle on material properties describing the inner region. To derive analytic forms for this dependence, we also perform the match in the limit of $\Gamma_s \to 0$ using a regular perturbation approach. Second, once the boundary conditions for (2.11) are known from matching, we examine the dynamic behaviour of the macroscopic contact angle as a function of Ca and ε for a range of transfer fluxes. The results show that surfactant transfer introduces a rich dynamic behaviour, not observed in either no-transfer or surfactant-free systems.

3.1. *Matching in the case of arbitrary* Γ_s

As is standard practice, we write the intermediate solution in Taylor series as $Ca \to 0$ holding r fixed:

$$\beta \sim \beta|_{\xi=0} + \left.\frac{f}{\sigma}\right|_{\xi=0} Ca \ln r, \quad \sigma \sim \sigma|_{\xi=0} + h|_{\xi=0} Ca \ln r. \tag{3.1a, b}$$

This has to match the outer solution as $r \to 0$:

$$\theta_{out} \sim \{\omega_0(\Gamma_s) + O(r)\} + O(Ca), \quad \sigma_{out} \sim \sigma_{m0}(t;\Gamma_s) + O(Ca). \tag{3.2a, b}$$

Briefly, the outer solution is static to $O(1)$ as $Ca \to 0$ because viscous effects are zero at this order. It follows that the interface has a static-like shape and that the surface tension (and therefore Γ) must be uniform on the free surface. Consequently, σ_{m0} is at most a function of time. The outer, static shape would intersect the solid with contact angle ω_0, which is largely determined by the intermediate-region hydrodynamics. This leads to behaviour (3.2) as $r \to 0$ (Cox 1986*b*; Dussan V. *et al.* 1991). From (2.4) and the equation of state (2.5) we can derive expressions for $\sigma_{m0}(t;\Gamma_s)$; for example, in the case of 'steady outer region',

$$\sigma_{m0}(t;\Gamma_s) = 1, \tag{3.3}$$

whereas for 'fixed interface length',

$$\sigma_{m0}(t;\Gamma_s) = 1 - \gamma\Gamma_s t/L_{ini}. \tag{3.4}$$

In general, however, $\sigma_{m0}(t;\Gamma_s)$ may follow any arbitrary time dependence.

Comparing (3.1) with (3.2), and recalling that $\theta \sim \beta + Ca\,\mathrm{d}\beta/\mathrm{d}\xi$, we deduce initial conditions

$$\sigma = \sigma_{m0}(t;\Gamma_s), \quad \beta = \omega_0(\Gamma_s) \quad \text{at} \quad \xi = 0. \tag{3.5a, b}$$

Similarly, matching the intermediate solution to the inner-region solution (see Cox 1986a, b) gives boundary conditions for the intermediate region at the edge of the inner region:

$$\sigma = \sigma_i, \quad \beta = \Theta_i \quad \text{at} \quad \xi = -\eta \quad (\equiv Ca \ln(L_i/L_o)),$$

where Θ_i and σ_i are the leading-order contact angle and surface tension in the inner region as $Ca \to 0$. These conditions allow one to integrate equations (2.11a, b). Once these equations are solved, we can construct a uniformly valid composite solution for the interface shape:

$$\theta \sim \beta(Ca \ln r; \Gamma_s) + f_0(r; \omega_0, \sigma_{m0}(t)) - \omega_0, \tag{3.6}$$

where $f_0(r; \omega_0, \sigma_{m0})$ denotes a static interface shape with contact angle ω_0 as in equation (1.2).

3.2. *Matching in the case $\Gamma_s \ll 1$*

The intermediate solution, expanded for small Γ_s as in § 2.4,

$$\beta - \{\beta_0 + \Gamma_s\beta_1 + O(\Gamma_s^2)\} + O(Ca), \quad \sigma \sim \{\sigma_0 + \Gamma_s\sigma_1 + O(\Gamma_s^2)\} + O(Ca), \tag{3.7a, b}$$

must match the following outer expressions, obtained by expanding (3.2) asymptotically as $\Gamma_s \to 0$ and valid as $r \to 0$:

$$\theta_{out} \sim \{\omega_{00} + \Gamma_s\omega_{01} + O(\Gamma_s^2) + O(r)\} + O(Ca), \tag{3.8a}$$

$$\sigma_{out} \sim \{\sigma_{m00}(t) + \Gamma_s\sigma_{m01}(t) + O(\Gamma_s^2)\} + O(Ca), \tag{3.8b}$$

and the following inner limiting forms as $r/\varepsilon \to \infty$:

$$\theta_i \sim \{\Theta_{i,00} + \Gamma_s\Theta_{i,01} + O(\Gamma_s^2)\} + O(Ca), \quad \sigma_i \sim \{\sigma_{i,00} + \Gamma_s\sigma_{i,01} + O(\Gamma_s^2)\} + O(Ca). \tag{3.8c, d}$$

Since $\Theta_i = \Phi(U, \Gamma_{CL}) \sim \{\Theta_{i,00} + \Gamma_s\Theta_{i,01} + O(\Gamma_s^2)\}$ and $\Gamma_{CL} \sim \{\Gamma_{i,00}(t) + \Gamma_s\Gamma_{i,01}(t) + \ldots\} + O(Ca)$ as $\Gamma_s \to 0$ in the inner region, we obtain $\Theta_{i,00} \equiv \Phi(U, \Gamma_{i,00})$ and $\Theta_{i,01} \equiv \partial\Phi/\partial\Gamma_{CL}|_{U,\Gamma_{i,00}}\Gamma_{i,01}$.

From equations (3.3) and (3.4) we deduce $\sigma_{m00}(t) = 1$, and either $\sigma_{m01}(t) = 0$ for a steady outer region, or $\sigma_{m01}(t) = -\gamma t/L_{ini}$ for a fixed spread surfactant area (provided $\Gamma_s\gamma t/L_{ini} \ll 1$).

Matching at each order in Γ_s gives

$O(1)$:

$$\text{Outer–intermediate} \qquad G_0(\omega_{00}) = K_{\theta 0}/K_{\sigma 0}, \quad K_{\sigma 0} = \frac{\sin\omega_{00}}{\omega_{00}}, \tag{3.9a, b}$$

$$\text{Inner–intermediate} \qquad K_{\sigma 0}G_0(\Theta_{i,00}) = K_{\theta 0} + Ca\ln(L_i/L_o), \quad K_{\sigma 0} = \frac{\sin\Theta_{i,00}}{\Theta_{i,00}}\sigma_{i,00}, \tag{3.9c, d}$$

where we have used the expressions for β_0 and σ_0 given in (2.13) and (2.14).

$O(\Gamma_s)$:

$$\text{Outer–intermediate} \qquad \beta_1(\omega_{00}) = \omega_{01}, \quad \sigma_1(\omega_{00}) = \sigma_{m01}(t). \tag{3.10a, b}$$

$$\text{Inner–intermediate} \qquad \beta_1(\Theta_{i,00}) = \Theta_{i,01}, \quad \sigma_1(\Theta_{i,00}) = \sigma_{i,01}. \tag{3.10c, d}$$

This shows that, to lowest order in Ca, and for $\Gamma_s \ll 1$, the outer interface is still static with contact angle equal to $\omega_{00} + \Gamma_s\omega_{01}$. Thus, the apparent dynamic contact angle receives an extra contribution, $\Gamma_s\omega_{01}$, owing only to the fact that surfactant

transfer is turned on. This contribution comes from the extra fluid motion which the transfer drives in the intermediate region.

3.3. *Relationship between the matching constants appearing in the general and in the $\Gamma_s \ll 1$ cases*

Using (2.18*a*, *b*) it is straightforward to show that

$$\sigma|_{\xi=0} = 1 + \Gamma_s \left[\pm 5 \frac{K_{\sigma 0}}{K_{\Gamma 0}} + K_{\sigma 1} \left(\frac{18 + \omega_{00}^2}{18} \right) \right], \tag{3.11a}$$

$$\omega_0 = \omega_{00} \left\{ 1 - \Gamma_s \left[\pm \frac{2}{K_{\Gamma 0}} + \frac{K_{\sigma 1}}{3K_{\sigma 0}} \right] \right\}. \tag{3.11b}$$

In order to find the dependence of $K_{\sigma 0}$, $K_{\sigma 1}$, ω_{00}, ω_{01} on ω_0, we iterate by first assuming $\omega_{00} = \omega_0$. Then we evaluate

$$K_{\sigma 0} = \sin \omega_{00}/\omega_{00}, \quad K_{\sigma 1} = \left[\sigma_{m01} \mp 5 \frac{K_{\sigma 0}}{K_{\Gamma 0}} \right] \frac{18}{18 + \omega_{00}^2}$$

from equations (2.18*a*) and (3.10*b*), where $K_{\Gamma 0} \equiv 1 + (K_{\sigma 0} - 1)/\gamma$. The final step is to update

$$\omega_{00} = \omega_0 \left\{ 1 - \Gamma_s \left[\pm \frac{2}{K_{\Gamma 0}} + \frac{K_{\sigma 1}}{3K_{\sigma 0}} \right] \right\}^{-1}$$

from (2.18*b*). ω_{01} may be found from $\omega_0 = \omega_{00} + \Gamma_s \omega_{01}$.

3.4. *Identifying parameters controlling the outer region*

In order to identify how inner parameters determine macroscopic quantities, we examine a situation where the material properties, $\Theta_i(U, \Gamma_{CL})$, $\sigma(\Gamma)$ and ε are known, and Γ_s has been measured (see § 3.7). Knowledge of these material properties, Ca, and the user-defined protocol for controlling the surface tension in the outer region is sufficient to determine the problem. We restrict our attention to $\Gamma_s \ll 1$ because this case has an analytic approximate solution valid when $\beta \to 0$ which allows us to extract explicit relations between the inner parameters and macroscopic quantities.

Using the results (3.9) and (3.10) of the match of the intermediate with the inner and the outer regions, and assuming that the angles, $\Theta_{i,00}$, ω_{00}, are small, it is easy to show that at $O(1)$

$$G_0(\Theta_{i,00}) = G_0(\omega_{00}) + \frac{1}{K_{\sigma 0}} Ca \ln \varepsilon, \tag{3.12a}$$

$$\frac{1}{\sigma_{m00}} \frac{\omega_{00}}{\sin \omega_{00}} = \frac{1}{\sigma_{i,00}} \frac{\Theta_{i,00}}{\sin \Theta_{i,00}}. \tag{3.12b}$$

Three additional relations are needed to determine all the variables: the equation of state, which we use to relate $\sigma_{i,00}$ to $\Gamma_{i,00}$, equation (3.9*b*), namely $K_{\sigma 0} = \sin \omega_{00}/\omega_{00}$, and the constitutive relation $\Theta_{i,00} = \Phi(U, \Gamma_{i,00})$. Results (3.12) had been obtained by Cox (1986*b*), but his interpretation differs from ours.

The leading behaviour of G_0 as $\omega_{00} \to 0$ is $G_0(\omega_{00}) \sim \omega_{00}^3/18$. This implies that, when surfactant does not transfer, and as long as the surface tension in the outer region is held constant (implying that $K_{\sigma 0}$ does not change with time), the apparent dynamic

contact angle behaves as $\omega_{00}^3 + \text{const} \sim 18Ca$, not too different from $\omega_0^3 + \text{const} \sim 9Ca$ for the surfactant-free case.†

At $O(\Gamma_s)$:

$$G_0\left[\frac{\Theta_{i,01}}{\pm 2/K_{\Gamma 0} + K_{\sigma 1}/3K_{\sigma 0}}\right] = G_0\left[\frac{\omega_{01}}{\pm 2/K_{\Gamma 0} + K_{\sigma 1}/3K_{\sigma 0}}\right] - Ca\,\ln\varepsilon, \tag{3.13a}$$

$$\sigma_{m01} = \pm 5\frac{K_{\sigma 0}}{K_{\Gamma 0}} + K_{\sigma 1}\left[1 + \frac{\omega_{00}^2}{18}\right], \quad \sigma_{i,01} = \pm 5\frac{K_{\sigma 0}}{K_{\Gamma 0}} + K_{\sigma 1}\left[1 + \frac{\Theta_{i,00}^2}{18}\right]. \tag{3.13b,c}$$

Since $K_{\Gamma 0} = 1 + (K_{\sigma 0} - 1)/\gamma$ from equation (2.5), σ_{m01} is known from the outer solution, and $\Theta_{i,01}$ is assumed known, equations (3.13) determine ω_{01}, $\sigma_{i,01}$, $K_{\sigma 1}$. Thus, (3.12) and (3.13) show that, when the transfer occurs, the macroscopic interface depends on $\omega_0 = \omega_{00} + \Gamma_s\omega_{01}$, through the parameters:

$$G_0(\Theta_{i,00}) - \frac{1}{K_{\sigma 0}}Ca\ln\varepsilon, \quad G_0\left[\frac{\Theta_{i,01}}{\pm 2/K_{\Gamma 0} + K_{\sigma 1}/3K_{\sigma 0}}\right] + Ca\ln\varepsilon. \tag{3.14a,b}$$

These parameters are modulated by information coming from the outer region via $\sigma_{m01}(t)$. Thus, in a manner equivalent to the surfactant-free case, the macroscopic interface shape depends on Θ_i and $Ca\ln\varepsilon$ through the apparent contact angle $\omega_{00} + \Gamma_s\omega_{01}$. However, here the inner contact angle Θ_i depends on the concentration at the contact line, Γ_{CL}, which in turn depends on the outer surface concentration $\sigma_{m0}(t)$. This information feedback from the outer region through $\sigma_{m0}(t)$ did not appear in the pure-fluid problem.

3.5. *Advancing contact angle vs. Ca*

3.5.1. $\Theta_i = 38^\circ$

We now integrate equations (2.11*a*, *b*) using the boundary conditions derived in § 3.1 and for given γ and Γ_s. We assume that the contact angle Θ_i is a known material property, and that the surface tension is controlled in the outer region as discussed in § 2.1. Therefore, our boundary conditions are

$$\beta = \Theta_i \quad \text{at} \quad \xi = -\eta \quad \text{and} \quad \sigma = \sigma_{m0}(t) \quad \text{at} \quad \xi = 0.$$

The chief result is the apparent contact angle ω_0, i.e. the slope at $\xi = 0$; and less importantly, the surface tension at $\xi = -\eta$. The equations are integrated as an initial value problem using a fourth-order Runge–Kutta method. Since the equations are autonomous, we may fix the origin of ξ arbitrarily. Thus, we define the auxiliary integration variable $\xi' \equiv \xi + \eta$ and start the integration at $\xi' = 0$ with $\beta = \Theta_i$ and an assumed $\sigma = \sigma_i$. We integrate until $\sigma = \sigma_{m0}(t)$, at which point $\xi' = \eta$ and $\beta = \omega_0$. If the condition $\sigma = \sigma_{m0}(\omega_0)$ cannot be met, we choose another initial σ_i until a map is built of permissible initial values σ_i. We illustrate the case with $\Theta_i = 38^\circ$ at steady state, which requires a constant outer surface tension, $\sigma_{m0}(\omega_0) = 1$. We chose $\gamma = -100$ as a typical value, corresponding to an almost 'solid' monolayer.

Before discussing the behaviour of the apparent dynamic contact angle, we note that multiple solutions are possible for certain $\Gamma_s > 0$ (i.e. surfactant transfers from the interface onto the solid). Figure 2 shows that there are two possible solutions to this boundary value problem, each having a different inner surface tension $\sigma_i = \sigma(-\eta)$.

† This leading behaviour of G_0 is accurate to within 2% only for $\omega_{00} < 30^\circ$. This limits the applicability of this scaling law to very small Ca. For comparison, consider that in the surfactant-free case the corresponding leading behaviour $g_{pure}(\omega_0) \sim \omega_0^3/9$ is accurate to within 2% for $\omega_0 < 120^\circ$.

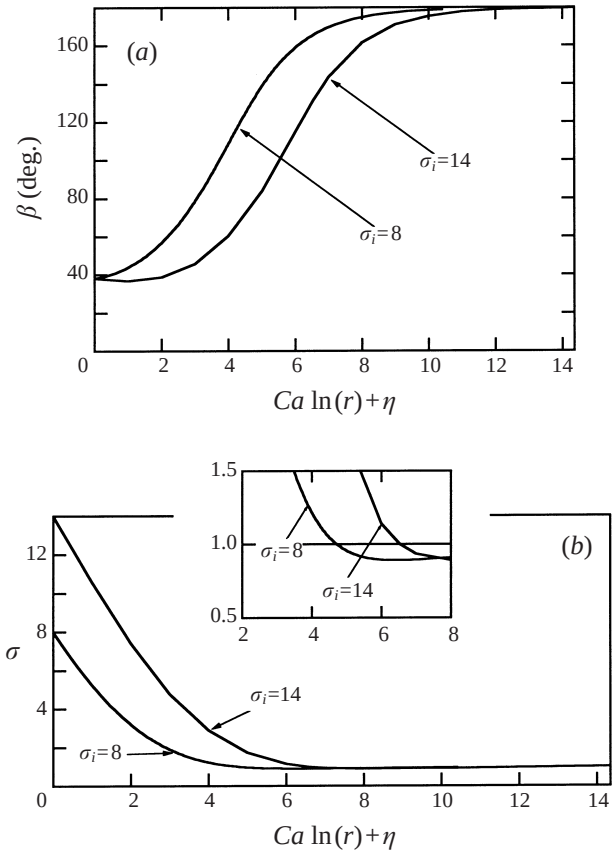

FIGURE 2. Interface slope (*a*) and surface tension (*b*) in the intermediate region, for two values of σ_i, and $\Gamma_s = 0.97$. Both solutions have the same macroscopic contact angle of about 131°, attained where the surface tensions equal 1; and the same inner contact angle, $\Theta_i = 38°$. This happens for pairs (σ_i, η): (14, −6.53) and (8, −4.75). For transfer rates above a critical value, a given system can exhibit two solutions satisfying the same boundary conditions.

In one of the solutions, the interface slope increases monotonically, whereas in the other it has a minimum near the inner region. As a result, two branches of ω_0 vs. η appear, both of which satisfy the outer condition $\sigma(0) = 1$. Thus, a given apparent contact angle appears at two different values of η.

Motivated by this observation, we calculate maps of ω_0 vs. η at several transfer fluxes, $\Gamma_s > 0$. Figure 3(*a*, *b*) shows the dependence of ω_0 and σ_i upon $Ca \ln \varepsilon$. For each pair $\{\sigma_i, Ca \ln \varepsilon\}$, the conditions at $\xi = 0$ (i.e. at the edge of the outer region) are $\beta = \omega_0$ and $\sigma = 1$. Before continuing with the discussion, we note that the lines that reach 180° do so at $Ca = \infty$. This is an artifact caused by our neglect of the motion of the displaced phase. This neglect is a good approximation for viscosity ratios $\mu_{gas}/\mu_{liq} \ll 1$ but only for $\omega_0 \neq 180°$, for then the stresses in the displaced phase are indeed negligible. However, as the displaced phase is squeezed against the solid (i.e. when $\beta \sim 180°$), the stresses in that phase are no longer negligible, signalling the presence of a singular limit when $\mu_{gas}/\mu_{liq} \to 0$ and $\beta \to 180°$. Cox (1986*b*) solved the problem with $\mu_{gas}/\mu_{liq} \neq 0$, but only for zero surfactant transfer; for a displaced phase of finite viscosity, he showed that the apparent contact angle attains 180° at Ca finite. As μ_{gas}/μ_{liq} decreases, the solution with $\mu_{gas}/\mu_{liq} = 0$ breaks down at β progressively

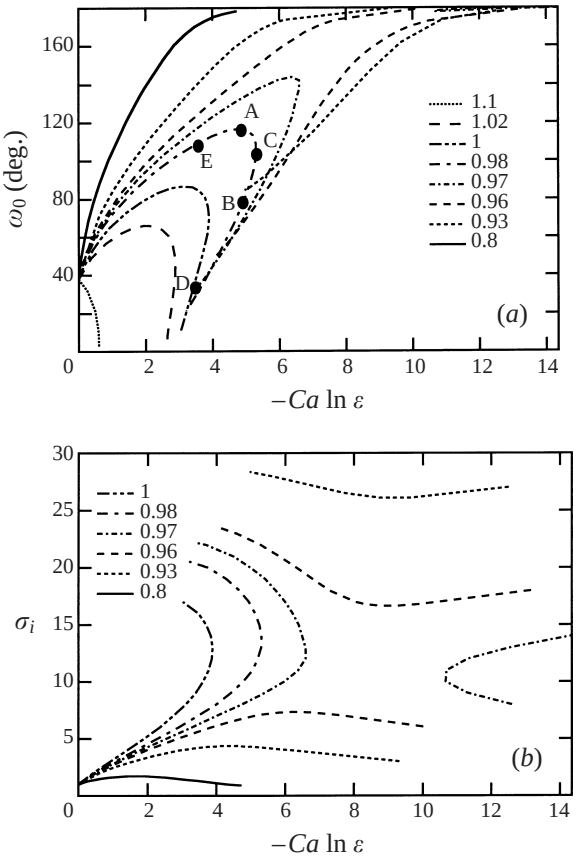

FIGURE 3. Advancing apparent contact angle (*a*) and inner surface tension (*b*) vs. $\eta = -Ca \ln \varepsilon$ for the values of $\Gamma_s > 0$ marked. Surfactant moves from the interface onto the solid. A viscous fluid displaces a passive gas phase. $\Theta_i = 38°$.

closer to 180° (or equivalently, at progressively larger Ca). Based on Cox's result, we can safely assume that our theory is good for $\beta \ll 180°$; and when $\beta \sim 180°$, the apparent contact angle should reach 180° at $Ca = Ca_{180}(\Gamma_s)$ with Ca_{180} increasing as $\mu_{gas}/\mu_{liq} \to 0$.

The behaviour of surfactant systems with transfer is much more complex than that of surfactant-free or no-transfer surfactant systems. In these simpler cases, ω_0 vs. $Ca \ln \varepsilon$ is a unique, single-valued function for each Θ_i, given by equation (1.1) for pure fluids and by equation (1.1) with g_{pure} replaced by G_0 from equation (2.15) for surfactants with no transfer.

As expected, surfactant systems at low transfer rates behave similarly to the no-transfer system. Their two most salient features appear at higher finite transfer rates: (i) above a certain Γ_s, two branches develop, implying that the same apparent contact angle will be seen at two different Ca for a given material system. Or, conversely, for a fixed Ca, the same apparent contact angle will be seen for two different macroscopic lengths, L_o. The implied hysteresis suggests that the apparent contact angles in the higher branch might be observed during increasing Ca, whereas those in the lower branch might be observed during decreasing Ca. We expect that our results should remain valid as long as ω_0 is not too close to 180°. (ii) as the transfer rate increases

further, the two branches close before reaching 180°; here our theory should remain valid for all ω_0. Thus, for $\Gamma_s \gtrsim 0.97$, apparent contact angles $\omega_0 \gtrsim 144°$ will not be observed, no matter how high Ca. Taking the case $\Gamma_s = 0.97$ for illustration, we note that ω_0 reaches a maximum at $Ca = Ca^*$ (point A in figure 3). At $Ca > Ca^*$, the steady solutions with $\mathrm{d}\omega_0/\mathrm{d}Ca < 0$ are likely to be unstable, so that increasing Ca beyond Ca^* would put the system on the (stable) lower branch of the curve where $\mathrm{d}\omega_0/\mathrm{d}Ca > 0$ (point B). Increasing Ca will evolve the system along the lower branch towards point C, where a further increase in Ca will fail to yield a steady flow. If Ca decreases having started on the higher branch at $Ca < Ca^*$ (i.e. to the left of A), the system will slow down along the higher branch. If the system had jumped to B, a decrease in Ca will slow the system down along the lower branch until it reaches the end point D, where a further decrease in Ca will not evolve a new steady solution. It is not clear whether the system will jump to point E and follow a sequence of steady solutions along the upper branch to $Ca = 0$, or continue to evolve through a set of unsteady flows. The hysteresis suggested by the steady calculations may be extended to unsteady flows by using $\sigma_m > 1$ to account for the depletion of the surface concentration by surfactant deposition. It remains to determine whether or not the non-uniqueness found here and that predicted in Chesters & Elyousfi's (1998) calculations of flow in a capillary tube are part of the same phenomenon.

3.5.2. $\Theta_i = 0$

In anticipation of our analysis of the inner region using the small-slope approximation, to be presented in § 4, here we discuss the dynamics of the intermediate region for $\Theta_i = 0$. This value of Θ_i is required for matching to any inner model based on the lubrication approximation because the slope of any 'small slope' inner region is always zero when viewed from the outer length scale.

Figure 4(*a*, *b*) shows that the striking difference from the case $\Theta_i = 38°$ is the absence of multiple solutions for a given contact angle. However, a similarity is still present in that, above a certain Γ_s, the range of available ω_0 is reduced. When $\Gamma_s \gtrsim 0.91$, the range of contact angles delivered by the inner region shrinks monotonically until it vanishes at $\Gamma_s = 1$. The dashed line in figure 4(*a*) is an attempt to show this shrinking trend: to the right of this line no steady solutions exist. At $\Gamma_s = 1$, the only point in parameter space for which a steady solution exists is $\{\omega_0 = 0, \eta = 0, \sigma = 1\}$, but this solution yields an interface shape of 'zero measure'.

We note that, when $\Theta_i = 0$, the surface tension, interface shape and surface velocity are approximately described by

$$\frac{\partial \sigma}{\partial \xi} \sim \frac{2}{\beta}(1 + 2u_i) + 4u_1 + \cdots, \tag{3.15a}$$

$$\frac{\partial \beta}{\partial \xi} \sim \frac{6}{\sigma_i \beta^2}(1 + u_i) + \frac{6}{\sigma_i^2 \beta}[\sigma_i u_1 - \sigma_1(1 + u_i)] + \cdots, \tag{3.15b}$$

$$\frac{\partial u_\tau}{\partial \xi} = -\frac{u_\tau}{\Gamma}\frac{1}{\gamma}\frac{\partial \sigma}{\partial \xi}, \tag{3.15c}$$

as $\beta \to 0$, $\xi \to -\eta$, $-\eta \leqslant \xi \leqslant 0$, where $u_\tau \sim u_i + \beta u_1 + \cdots$ and $\sigma \sim \sigma_i + \beta\sigma_1 + \cdots$.

We are interested in the behaviour of ω_0, which may be thought of as β evaluated at $\xi = -\eta = Ca \ln \varepsilon$. When $u_i \neq -1$, the usual behaviour, $\omega_0 \sim (18\, Ca \ln(\varepsilon^{-1}))^{1/3}$,

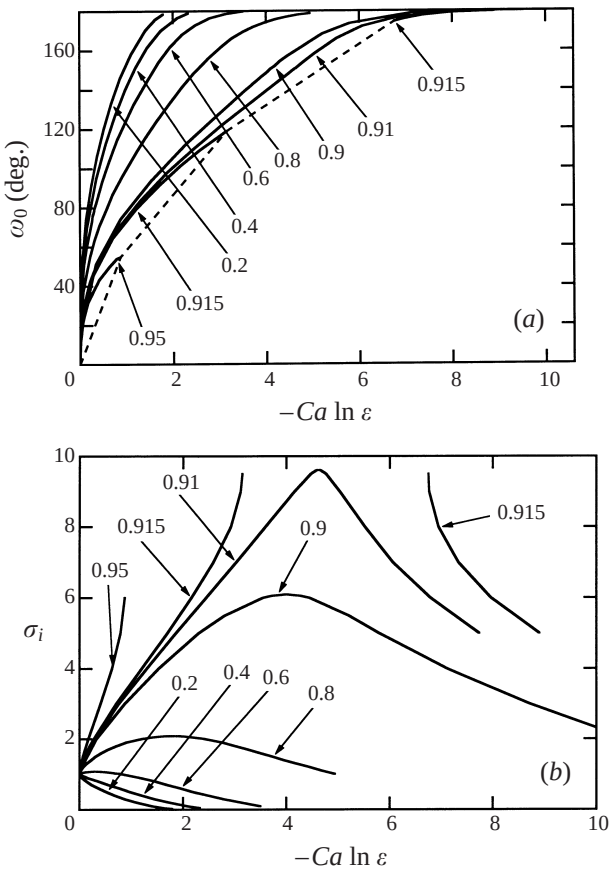

FIGURE 4. As figure 3 but for $\Theta_i = 0°$. Dashed line: boundary for existence of steady solutions.

prevails. However, when $u_i = -1$ the leading term of the Taylor series for β, equation (3.15*b*) vanishes and the apparent contact angle depends on a different power of Ca:

$$\omega_0 \sim [12u_1\sigma_i^{-1}Ca\ln(\varepsilon^{-1})]^{1/2}, \tag{3.16a}$$

where

$$u_1 = \pm(-\sigma_i/3\gamma\Gamma_i)^{1/2}. \tag{3.16b}$$

Thus, since the Marangoni number $M = \gamma/Ca$, we may write

$$\omega_0 \sim [12(-\gamma/3\sigma_i\Gamma_i)^{1/2}(-M)^{-1}\ln(\varepsilon^{-1})]^{1/2}. \tag{3.17}$$

Thus, when $u_i = -1$, the Marangoni effect plays a role in the dynamic contact angle, in qualitative agreement with the result of Joanny (1989). Equations (3.16) and (3.17) imply that, in order that ω_0 be real, $u_1 > 0$. Finally, equation (3.15*b*) suggests that, if $\beta > 0$, $\sigma_i > 0$ and $\xi + \eta > 0$, then at the edge of the inner region $u_i > -1$. This condition indicates that, at steady state and when $\Theta_i = 0$, the transfer ratio cannot exceed unity.

3.6. *Receding contact angle:* $\Theta_i = 120°$

Figure 5 shows the receding contact angle for various surfactant transfer fluxes from the solid to the interface, $\Gamma_s < 0$. For this case to occur, surfactant adsorbed on

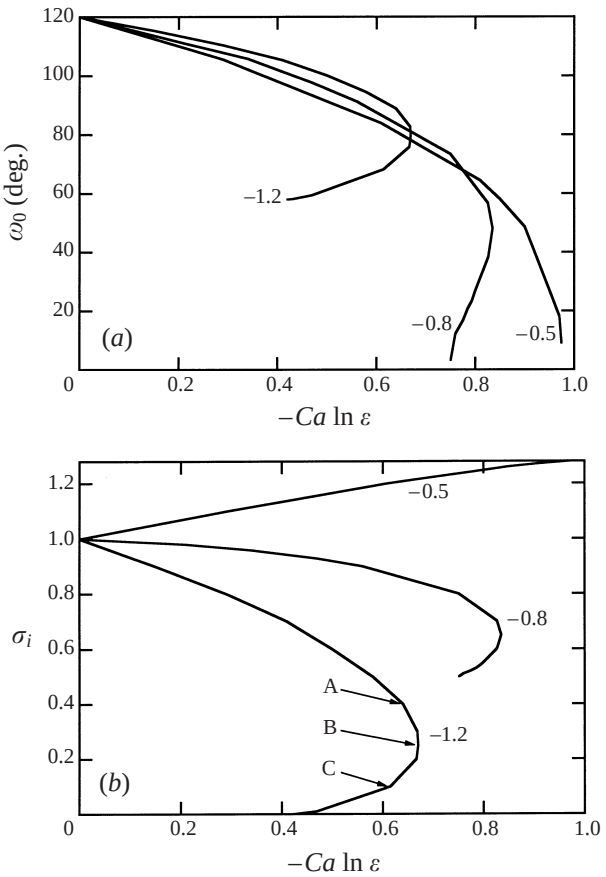

FIGURE 5. Receding apparent contact angle (a) and inner surface tension (b) vs. $\eta = -Ca \ln \varepsilon$ for the values of $\Gamma_s < 0$ marked. Surfactant moves from the solid onto the interface. A viscous fluid is displaced by a passive gas phase. $\Theta_i = 120°$.

the solid must be able to desorb onto the interface as the solid emerges from the liquid. This may happen for instance if the adsorption and desorption took place in two different liquids having respectively less and more affinity for the surfactant than the solid. For small $\Gamma_s < 0$ the receding contact angle decreases monotonically with $-Ca \ln \varepsilon$ until it reaches zero. This is consistent with the general behaviour of receding motion. However, when $\Gamma_s < \Gamma_s^{crit} < 0$, a range of $Ca \ln \varepsilon$ develops where two contact angles appear for each $Ca \ln \varepsilon$. At first the receding angle still decreases to zero ($\Gamma_s = -0.8$), but, for sufficiently large $|\Gamma_s|$, ω_0 remains above a minimum. The lower branch where the angle increases with $-Ca \ln \varepsilon$ is probably unstable.

The explanation for the change in behaviour is found by examining the interface shapes and surface tension profiles near the turnaround, point B in figure 5(b). From A to B to C, the initial surface tension σ_i decreases monotonically. Figure 6 shows that the end point $\sigma = 1$, which determines the value of $Ca \ln \varepsilon$, increases from A to B but decreases from B to C. The reason lies in the coupling between equations (2.11a, b). When σ_i is small (0.1 in the example) β decreases initially very rapidly by equation (2.11a). This raises the shear stress so much that the growth rate of the surface tension overtakes the cases with larger σ_i. By the time β decreases less rapidly,

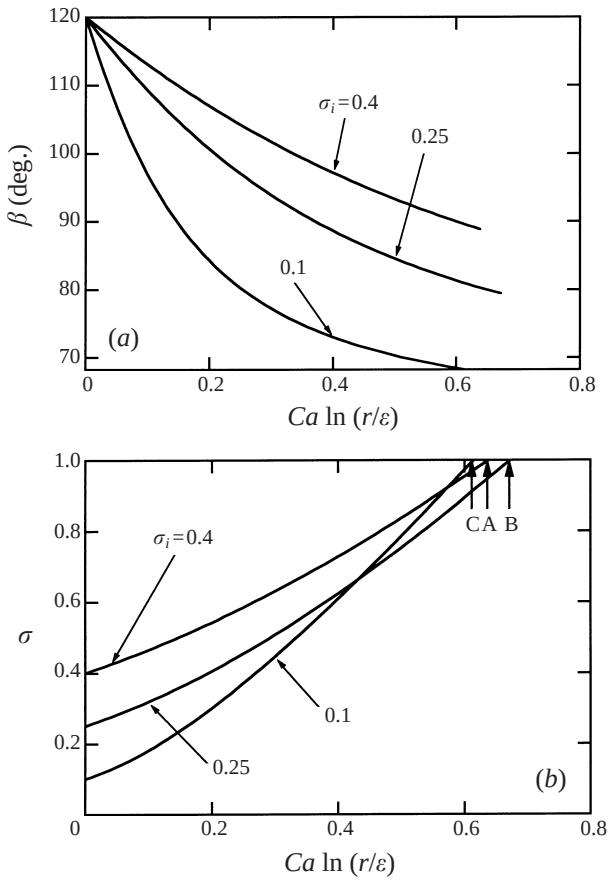

FIGURE 6. Interface shape (*a*) and surface tension profile (*b*) for points A, B and C of case $\Gamma_s = -1.2$ in figure 5(*b*).

σ is too close to 1. Consequently, for σ_i small enough, the end point $\sigma = 1$ is achieved at a smaller $-Ca \ln \varepsilon$.

3.7. *Suggested method for measuring* ω_0

Assuming that we can optically image the interface in the region described by equation (3.6), and since Γ_s and γ are both known by independent measurements (Γ_s can be found from $L(t) = L_{ini} - \Gamma_s t$, where $L(t)$ is controlled so as to keep the surface tension constant in the outer region), ω_0 could be measured (and the theory tested) by a process similar to that used for pure fluids (Dussan V. *et al.* 1991). This process uses ω_0 as a fitting parameter that minimizes the square differences between theory (equation (3.6)) and experiment. Of course, merely minimizing this square difference does not guarantee that a 'good' value of ω_0 has been found. Another necessary condition is that the data be uniformly scattered around the best fit, i.e. that no systematic deviations be present (Marsh *et al.* 1993).

4. Can surface diffusivity allow surfactant transfer?

In this section we analyse a model for the inner region where slip on the solid alleviates the stress singularity and surface diffusivity, D_s, on the interface allows

surfactant transfer. In order to allow analytical treatment, we assume that, in the inner region, the interface slope relative to the solid is small so that lubrication theory may be used. Scaling arguments, not subject to small-slope limitations, are shown in the Appendix. In this section we use x, y Cartesian axes with x along the solid and y perpendicular to it and into the liquid. The solid is at $y = 0$ and the contact line position is (0, 0).

The evolution equations for Γ and the interface height h vary according to the slip model chosen. For example, by prescribing a slip velocity with characteristic length λ in dimensional form as $u|_{y=0} = Ux/(x + \lambda)$ (Dussan V. 1976), and using length scales $h \sim \lambda Ca^{1/3}$ and $x \sim \lambda$, the dimensionless evolution equations are

$$\frac{\bar{x}}{\bar{x}+1} + \sigma h_{\bar{x}\bar{x}\bar{x}} \frac{h^2}{3} + M\,Ca^{1/3}\Gamma_{\bar{x}} \frac{h}{2} = 0, \tag{4.1}$$

$$\Gamma \left[\frac{\bar{x}}{\bar{x}+1} + \sigma h_{\bar{x}\bar{x}\bar{x}} \frac{h^2}{2} + M\,Ca^{1/3}\Gamma_{\bar{x}} h \right] - \Gamma_{\bar{x}} Pe_s^{-1} + \Gamma_s = 0. \tag{4.2}$$

The boundary conditions are

$$h = 0, \quad \mathrm{d}h/\mathrm{d}\bar{x} = \phi \quad \text{at} \quad \bar{x} = 0; \quad h \to \infty, \quad \mathrm{d}\Gamma/\mathrm{d}\bar{x} \to 0 \quad \text{as} \quad \bar{x} \to \infty. \tag{4.3a–d}$$

Subscript '$\bar{x}$' denotes differentiation; $M = \gamma/Ca < 0$ is the Marangoni number, $Pe_s = U\lambda/D_s$ is a surface Péclet number and λ plays the role of L_i. Both Pe_s and $M\,Ca^{1/3}$ are $O(1)$ as $Ca \to 0$. The surfactant concentration on the solid, Γ_s, represents the dimensionless surfactant flux. We further assume that Γ_s is linearly related to the concentration on the free surface next to the solid, i.e. $\Gamma_s = k\Gamma(0)$, where k is a adsorption rate constant, and that $\sigma = 1 + \gamma(\Gamma - 1)$.

4.1. *Transport: small-$\bar{x}$ behaviour*

In order to investigate how slip and surface diffusivity affect the surfactant transport at the contact line, we first examine the small-$\bar{x}$ behaviour of equations (4.1) and (4.2). We assume that, for $\bar{x} \ll 1$, the variables may be expanded asymptotically as

$$h \sim \phi\bar{x} + (b + b_L \ln(\bar{x}))\bar{x}^2 + (c + c_L \ln(\bar{x}))\bar{x}^3 + \cdots, \tag{4.4}$$

$$\Gamma \sim \Gamma_0 + \Gamma_1\bar{x} + \Gamma_2\bar{x}^2 + \cdots, \tag{4.5}$$

where $\phi \equiv \theta/Ca^{1/3} = O(1)$ as $Ca \to 0$ and θ is the (small) contact angle. By substituting these expansions into equations (4.1) and (4.2), we find:

$$1 + \tfrac{1}{2}\phi\Gamma_1 M\,Ca^{1/3} + \tfrac{2}{3}\phi^2 b_L \sigma_0 = 0, \tag{4.6}$$

$$-1 + \tfrac{1}{2}M[b\Gamma_1 + 2\phi\Gamma_2] + \phi^2[\tfrac{2}{3}b_L\Gamma_1\gamma + \sigma_0(2c + \tfrac{11}{3}c_L)] + \tfrac{4}{3}\phi\sigma_0\, b\, b_L = 0, \tag{4.7}$$

$$\tfrac{1}{2}Mb_L\Gamma_1 + \phi\sigma_0(4b_L^2 + 6\phi c_L)/3 = 0, \tag{4.8}$$

$$\Gamma_s - \Gamma_1 Pe_s^{-1} = 0, \tag{4.9}$$

$$\Gamma_0(1 + \phi^2 b_L\sigma_0 + M\,Ca^{1/3}\phi\Gamma_1) - 2Pe_s^{-1}\Gamma_2 = 0. \tag{4.10}$$

Since mass is conserved at the contact line, the diffusive flux, Γ_1, is fixed by Γ_s and Pe_s in equation (4.9). The adsorption constant k then determines the concentration level Γ_0. Qualitatively similar results arise for the slip models of Navier (Goldstein 1965, pp. 676–680) and Greenspan (1978).

Thus, the details of the slip mechanism do not affect whether or not transfer takes place. Slip regularizes the stress by making the fluid velocity zero at the contact line, but this necessarily causes the surface concentration to blow up at the contact line if transport is purely convective. The only exception is the special no-transfer case analysed by Cox (1986*b*). In all transfer cases surface diffusivity has the double effect of relaxing the concentration growth rate and providing a mechanism of surfactant transfer.

4.2. *Large-$\bar{x}$ behaviour*

In order to connect the lubrication analysis to the model posed in § 2, we extract large-$\bar{x}$ asymptotic behaviours for equations (4.1) and (4.2). As in other lubrication models of advancing liquids, there are two possible asymptotic behaviours. In the first one, the interface height grows quadratically,

$$h \sim A\bar{x}^2 + B\bar{x} + C,$$

and the surface concentration approaches a constant,

$$\Gamma \sim \Gamma_\infty + 2(M\,Ca^{1/3}A\bar{x})^{-1}(2\Gamma_s/\Gamma_\infty - 1) \quad \text{as} \quad \bar{x} \to \infty.$$

This behaviour may be matched to a static outer region at low Ca, where the surface concentration is independent of position at lowest order in Ca. The second behaviour is logarithmic, and may be matched to the intermediate region of § 2. The logarithmic large-$\bar{x}$ behaviour of the inner solution, with both $\bar{x}$ and $\bar{h}$ made dimensionless by $L_i = \lambda$ (i.e. $h\,Ca^{1/3} = \bar{h}$), is

$$\bar{h}_{inner} \sim \bar{x}[18Ca\,\sigma_\infty^{-1}(1 - \Gamma_s/\Gamma_\infty)\ln(\bar{x})]^{1/3}, \tag{4.11}$$

$$\Gamma_{inner} \sim \Gamma_\infty + (M\,Ca)^{-1}(\tfrac{3}{2}\sigma_\infty)^{1/3}(1 - \Gamma_s/\Gamma_\infty)^{-1/3}(1 - 2\Gamma_s/\Gamma_\infty)(Ca\ln(\bar{x}))^{2/3}. \tag{4.12}$$

The variables, Γ_∞ and σ_∞, are related by the equation of state for the free surface, (2.5). Since these expressions are independent of Pe_s, mass transfer occurs only by convection at large $\bar{x}$. The interface slope is asymptotically $\beta \sim \bar{h}/\bar{x}$ as $\bar{x} \to \infty$:

$$\beta_{inner} \sim [18Ca\,\sigma_\infty^{-1}(1 - \Gamma_s/\Gamma_\infty)\ln(\bar{x})]^{1/3}. \tag{4.13}$$

These expressions should match to the intermediate region solution for $\Theta_i = 0$. We write the intermediate solution in inner variables, and expand in Taylor series as $Ca \to 0$ holding r/ε fixed. In this limit, $\beta \to 0$ so we may replace r/ε by $\bar{x}$ to a first approximation, to yield

$$\beta_{interm} \sim (18(1 + u_i)\sigma_i^{-1}Ca\ln(\bar{x}))^{1/3}, \tag{4.14}$$

$$\Gamma_{interm} \sim \Gamma_i + (M\,Ca)^{-1}(\tfrac{3}{2}\sigma_i)^{1/3}(1 + u_i)^{-1/3}(1 + 2u_i)(Ca\ln(\bar{x}))^{2/3}, \tag{4.15}$$

where u_i and Γ_i are unknown constants to be determined by matching. Recall that Γ_i and u_i are the initial values of surface concentration and interface velocity at $\xi = -\eta$ ($= Ca\ln\varepsilon$) in the intermediate region.

By comparing equations (4.12) and (4.13) to (4.15) and (4.14) we find values for the integration constants:

$$\Gamma_i = \Gamma_\infty, \tag{4.16}$$

$$\sigma_i = \sigma_\infty, \tag{4.17}$$

$$u_i = -\Gamma_s/\Gamma_\infty. \tag{4.18}$$

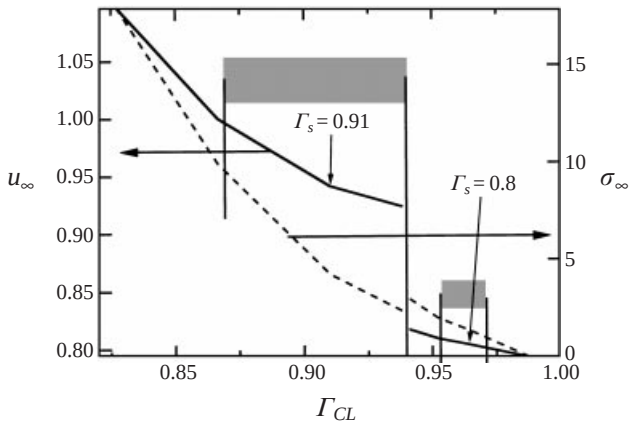

FIGURE 7. Inner-region model prediction of $u_\infty = \Gamma_s/\Gamma_\infty$ and σ_∞ for various contact line concentrations, Γ_{CL}, and for the two transfer ratios $\Gamma_s Pe_s^{-1} = 40$, $Ma\,Ca^{1/3} = -100$, $\gamma = -100$. Solid lines: u_∞; dashed lines: σ_∞. Shaded areas between vertical lines mark the regions of steady solutions as given by the intermediate-region solution at the respective transfer rate Γ_s, see figure 4.

Equation (4.18) simply expresses the mass balance between the transferred flux, Γ_s, and the convected flux in the no-diffusion region, Γu.

In order to relate Γ_∞ to the parameters of the problem, we solve for $\bar{h}$ and Γ by integrating (4.1) and (4.2) with boundary conditions (4.3*a*, *b*) and

$$\left.\begin{aligned} &\Gamma = \Gamma_{CL} && \text{at} \quad \bar{x} = 0, \\ &h \sim \bar{x}[18\sigma_\infty^{-1}(1 - \Gamma_s/\Gamma_\infty)\ln(\bar{x})]^{1/3} && \text{as} \quad \bar{x} \to \infty. \end{aligned}\right\} \tag{4.19}$$

The method consists of solving an initial value problem for given ϕ, $M\,Ca^{1/3}$, Pe_s, Γ_s and Γ_{CL}, with the condition at infinity replaced by $\mathrm{d}^2h/\mathrm{d}\bar{x}^2 = b$ at $\bar{x} = 0$. The value of b is varied until the behaviour (4.19) is obtained. Figure 7 shows results of a partial parameter search where Γ_{CL} determines the possible surface tensions to be passed on to the intermediate region for $\phi = 1$, $M\,Ca^{1/3} = -100$, $Pe_s = 1/40$. Clearly, to each Γ_s correspond values of Γ_∞ and σ_∞. By (4.17), σ_i is then fixed. However, the intermediate-region dynamics dictates the allowable ranges of σ_i for steady solutions. Thus, only material systems which can deliver surface tensions σ_i in these ranges will exhibit steady solutions.

5. Conclusions

We have identified quantities describing the macroscopic interface shape in a spreading liquid with an insoluble surfactant for the general case of surfactant exchange between the fluid–fluid and the solid–fluid interfaces. One of these quantities, which plays the role of an apparent dynamic contact angle, depends primarily upon parameters of the inner region. In this respect, the surfactant problem behaves analogously to the surfactant-free case. However, the surface concentration in the outer region (a variable that an operator can control and which dictates the concentration of surfactant in the inner region) indirectly affects the actual and the apparent dynamic contact angles. In this respect, the problem of spreading with surfactants differs significantly from the surfactant-free case where actions taken in the outer region do not affect the dynamic contact angle passed on to the outer region.

The contact-line singularity that has been widely examined in surfactant-free systems reappears with vengeance in systems with surfactants. Cox showed that, when surfactant does not transfer to the solid, i.e. it remains 'captive' on the fluid–fluid interface, the singularity may be removed by the same mechanisms as in surfactant-free systems. Chief among possible mechanisms is the assumption that fluids slip along the solid very close to the contact line. However, when surfactant transfers only by convection at the contact line, slip cannot remove the singularity because in doing so it would annihilate the surfactant transfer. Additional mechanisms such as surface diffusivity must be present. Alternatively, transfer may be accounted for at the interface level by assuming appropriate 'interphase' models where the 'interphase' region with the surfactant is modelled as an anisotropic three-dimensional phase, much in the spirit of Shikhmurzaev. Postulating that surface diffusivity accounts for the transfer does lead to a well-posed boundary value problem – at least in the limit $Ca \ll 1$, $UL_o/D_s \gg 1$. If one wished to define an effective surface velocity for the surfactant, $u_{eff} \equiv \Gamma^{-1}(-D_s \nabla_{II} \Gamma + \Gamma u_\tau)$, one could define a slip coefficient at the interface, $\lambda \equiv (u_{eff} - u_\tau)/\tau_w$, where τ_w is the shear stress at the free surface. Thus, it may prove difficult to distinguish between slip and surface diffusivity in an experiment unless these parameters can be independently characterized.

We derive matching conditions between the intermediate region and the outer and inner regions. The matching conditions may be used as boundary conditions for the solution of (2.11). One of these conditions fixes the interface slope; the other one fixes the surface tension. If the conditions are applied at the overlap between outer and intermediate regions, then they specify the apparent dynamic contact angle and the outer surface tension. In surfactant-free systems matching also provides the initial condition for the interface shape in the form of a dynamic contact angle; but because a closed-form solution exists for the shape, the contact angle is incorporated directly in the analytical solution. Though the macroscopic dynamic contact angle is ultimately determined in some complicated way by material parameters of the inner region, our approach hinges on measuring the dynamic contact angle experimentally rather than computing it from the inner parameters on which it depends.

For small transfer rates, Γ_s, we have identified relations between inner material parameters and the quantities characterizing the outer region. Because an analytical solution for arbitrary Γ_s is not available, we cannot identify, for arbitrary Γ_s, macroscopic parameters depending only on combinations of material properties, as has been done in the surfactant-free problem. For the special case $\Gamma_s = 0$ an exact solution exists and these combinations are expressed in equations (3.12). For arbitrary Γ_s, even the possibility of identifying such relations is not at all obvious; generalizing the theory for arbitrary Γ_s is a pending – perhaps impossible? – task. Nevertheless, it is possible to measure the macroscopic quantities ω_0 and σ_{m0} at any Γ_s and, should these measurements be successful, model the macroscopic dynamics of the spreading process.

We also examined the dynamics of the intermediate region. The behaviour of the apparent contact angle versus $Ca \ln \varepsilon$ is much richer than that of the no-surfactant or the no-transfer surfactant cases. These results suggest that, for some transfer rates, some apparent contact angles may not be reachable no matter what the value of Ca; steady solutions may fail to exist in certain ranges of Ca, and that hysteretic behaviour may develop during increasing–decreasing Ca-advancing cycles.

Finally, we proposed an approximate inner model where slip removes the stress singularity and surface diffusivity effects the surfactant transfer at the contact line. As with all small-slope models, $\Theta_i = 0$ because the slope is vanishingly small when seen from the large macroscopic length scale. Using the matching conditions between

the inner and intermediate regions derived in (3.1), we provide initial conditions for the intermediate region based on the dynamics of the inner region. We found that, in order for a steady state to develop, the inner-region parameters cannot be arbitrary but their ranges must meet certain constraints.

I wish to thank the following institutions for the financial and/or material support they provided during the different periods of time when this work was done: Department of Chemical Engineering, University of Pennsylvania; Schlumberger-Doll Research; NASA grant NAG3-1390; Carnegie Mellon University; NRC Associateship Program. I also wish to thank Arijit Bose, Elizabeth B. Dussan V. and S. Garoff for insightful and stimulating discussions. Finally, I am grateful to two anonymous reviewers for their critical comments and suggestions.

Appendix

We consider the inner-region flow in a straight wedge, with an insoluble surfactant on the free surface. The inner length is the slip length λ. The inner model is the same as in §4, except that the interface is assumed flat and its location is $\phi = \alpha$, with $\alpha = O(1)$. For simplicity we do not consider interface deformation; therefore, we do not satisfy the normal component of the dynamic boundary condition at the free surface. Because the discussion is not limited to small slopes, the small-slope approximation cannot be used to make analytical progress. Instead, we look for the scaling behaviour of the solution near the moving contact line and at large distances from it.

All lengths are made dimensionless by λ, concentrations by Γ^*, and velocities by U. In the inner region the flow (assumed steady) is Stokes'. The boundary conditions are

surfactant mass

$$-Pe_s^{-1}\,\mathrm{d}\Gamma/\mathrm{d}r + \Gamma u = q \quad \text{on} \quad \phi = \beta, \tag{A 1}$$

where the surfactant flux, q, is a constant;

tangential stress

$$\mathrm{d}\Gamma/\mathrm{d}r = M^{-1}(1/r)\partial u/\partial\phi \quad \text{on} \quad \phi = \beta; \tag{A 2}$$

slip at the solid wall (we assume a prescribed velocity à la Dussan V. (1976))

$$u = r/(1+r) \quad \text{on} \quad \phi = 0. \tag{A 3}$$

At the contact line, all the surfactant transported along the free surface must be removed by the solid after being adsorbed on it. This mass balance is expressed as $\Gamma_s = q$. The adsorption isotherm gives the solid concentration as $\Gamma_s = k\Gamma_0$ at the contact line. Since $q = \Gamma_s$ by mass conservation, it follows that $q = k\Gamma_0$.

Behaviour as $r \to 0$

If we assume

$$\Gamma \sim \Gamma_0 + r\Gamma_1 + r^2\Gamma_2 \ldots \quad \text{and} \quad u \sim ru_1(\phi) + r^2u_2(\phi) \quad \text{as} \quad r \to 0,$$

it is found upon substitution in (A 1)–(A 3) that

$$\begin{aligned} \mathrm{d}u_1/\mathrm{d}\phi &= -M\,Pe_s q \quad \text{at} \quad \phi = \beta, \\ \Gamma_1 &= M^{-1}\mathrm{d}u_1/\mathrm{d}\phi \quad \text{at} \quad \phi = \beta, \\ u_1 &= 1 \quad \text{at} \quad \phi = 0. \end{aligned}$$

From the linearity of Stokes' flow, the last two equations imply

$$u_1 = f_1(\phi) + qM\,Pe_s f_2(\phi), \tag{A 4}$$

where $\mathrm{d}f_1/\mathrm{d}\phi(\beta) = 0$ and $\mathrm{d}f_2/\mathrm{d}\phi(\beta) = 1$; $f_1(0) = 1$ and $f_2(0) = 0$. The structure $u \sim r$ is independent of the slip model chosen. Only the coefficient functions f_1 and f_2 change upon a change in slip model.

The surface concentration behaves as

$$\Gamma \sim \Gamma_0 - rqPe_s,$$

where Γ_0 is undetermined and must be found by matching to the outer region where the concentration can be controlled. Since $q = k\Gamma_0$, it follows that

$$\Gamma \sim \Gamma_0[1 - rkPe_s] \quad \text{as} \quad r \to 0.$$

From dimensional considerations, we conclude that all the powers r^n must be proportional to Γ_0, so that

$$\Gamma/\Gamma_0 = f(r, k, Pe_s).$$

At the next order, the expansions give

$$\Gamma_2 = -\tfrac{1}{2}Pe_s\Gamma_0 u_1(\beta) \quad \text{and} \quad \mathrm{d}u_2(\beta)/\mathrm{d}\phi = 2M\Gamma_2.$$

Therefore,

$$\mathrm{d}u_2(\beta)/\mathrm{d}\phi = -2M\,Pe_s\Gamma_0 u_1(\beta)$$

The convective flux is $q_{conv} = \Gamma u \sim r\Gamma_0 u_1(\beta)$. Thus only diffusion is present at small r.

Large-r behaviour

We now examine the large-r behaviour, corresponding to the physical distance being much larger than λ. Since, in this limit $u \sim 1$ on the solid, both convection and diffusion have the potential to be important. From (A 1) and (A 2), $\partial u/\partial\phi = -MPe_s r(-\Gamma u + q)$. This shows that, as $r \gg 1$, $\Gamma u \to q$. This statement implicitly assumes that $\partial u/\partial\phi$ remains $O(1)$ as $r \gg 1$; we will justify this *a posteriori*.

By the same reasoning, integration of (A 2) gives $\Gamma \to C_1 + M^{-1}\partial u/\partial\phi \ln(r)$ as $r \gg 1$. This, in turn, when combined with $\Gamma u \to q$, implies that, to lowest order in Ca, $u \to q/\Gamma = C_2$ as $r \gg 1$. Since both u and Γ approach constants as $r \gg 1$, the problem for the velocity and concentration fields may be matched to the problem we have solved in the absence of diffusion, i.e. when $Pe_s(L_o/\lambda) \gg 1$, outside the inner region. Now we can justify the assumption that $\partial u/\partial\phi =$ bounded as $r \gg 1$: since $u(\beta) \to C_2$ on the free surface, and $u(0) \to 1$ at the solid, it follows that $\partial u/\partial\phi \sim (C_2 - 1)/\beta$ as $r \to \infty$.

This analysis shows that a slip region with surface diffusivity such that $MPe_s = O(1)$ allows flux, q, to be specified externally. The model accounts for surfactant flux at $r = 0$, while it recovers the no-diffusion behaviour when $r \gg 1$. For this discussion we have assumed that $Pe_s = O(1)$ as $Ca \to 0$, which together with $MPe_s = O(1)$ implies that $M = O(1)$. This ordering is the same as that found in the small-slope analysis of § 4, where $M\,Ca^{1/3}$ and Pe_s are both $O(1)$, except that $Ca^{1/3}$ (which denotes the ratio of vertical to horizontal length scales in lubrication theory) is here replaced by 1.

REFERENCES

Abramowitz, M. & Stegun, I. A. 1972 *Handbook of Mathematical Functions*. Dover.

Adamson, A. W. 1967 *Physical Chemistry of Surfaces*. Interscience.

Blodgett, K. B. 1935 Films built by depositing successive monomolecular layers on a solid surface. *J. Am. Chem. Soc.* **57**, 1007.

Chen, Q., Ramé, E. & Garoff, S. 1995 The breakdown of asymptotic models of liquid spreading at increasing capillary number. *Phys. Fluids* **7**, 2631.

Chesters, A. K. & Elyousfi, A. B. A. 1998 The influence of surfactants on the hydrodynamics of surface wetting: I The nondiffusing limit. *J. Colloid Interface Sci.* **207**, 20.

Cox, R. G. 1986*a* The dynamics of the spreading of liquids on a solid surface. Part 1. Viscous flow. *J. Fluid Mech.* **168**, 169.

Cox, R. G. 1986*b* The dynamics of the spreading of liquids on a solid surface. Part 2. Surfactants. *J. Fluid Mech.* **168**, 195.

Damania, B. S. & Bose, A. 1986 Effects of surfactants in the spreading of liquids on solid surfaces, *J. Colloid Interface Sci.* **113**, 321.

Dussan V., E. B. 1979 On the spreading of liquids on solid surfaces: static and dynamic contact angles. *Ann. Rev. Fluid Mech.* **11**, 371.

Dussan V., E. B. 1976 The moving contact line: the slip boundary condition. *J. Fluid Mech.* **77**, 665.

Dussan V., E. B. & Davis, S. H. 1974 On the motion of a fluid–fluid interface along a solid surface. *J. Fluid Mech.* **65**, 71.

Dussan V., E. B., Ramé, E. & Garoff, S. 1991 On identifying the appropriate boundary conditions at a moving contact line: an experimental investigation. *J. Fluid Mech.* **230**, 97.

Finlow, D. E., Kota, P. R. & Bose, A. 1996 Investigation of wetting hydrodynamics using numerical simulations. *Phys. Fluids* **8**, 302.

Gennes, P. G. de 1985 Wetting: statics and dynamics. *Rev. Mod. Phys.* **57**, 827.

Goldstein, S. 1965 *Modern Developments in Fluid Dynamics*. Dover.

Greenspan, H. P. 1978 On the motion of a small viscous droplet that wets a surface. *J. Fluid Mech.* **84**, 125.

Hadjiconstantinou, N. G. 1999 Combining atomistic and continuum simulations of contact-line motion. *Phys. Rev.* E **59**(2), 2475.†

Hansen, R. J. & Toong, T. Y. 1971 Dynamic contact angle and its relationship to forces of hydrodynamic origin. *J. Colloid Interface Sci.* **37**, 196.

Hocking, L. M. 1977 A moving fluid interface. Part 2. The removal of the force singularity by a slip flow. *J. Fluid Mech.* **79**, 209.

Hocking, L. M. & Rivers, A. D. 1982 The spreading of a drop by capillary action. *J. Fluid Mech.* **121**, 425.

Huh, C. & Mason, S. G. 1977 The steady movement of a liquid meniscus in a capillary tube. *J. Fluid Mech.* **81**, 401.

Huh, C. & Scriven, L. E. 1971 Hydrodynamic model of steady movement of a solid/liquid/fluid contact line. *J. Colloid Interface Sci.* **35**, 85.

Joanny, J. F. 1989 Kinetics of spreading of a liquid supporting a surfactant monolayer: Repulsive solid surfaces. *J. Colloid Interface Sci.* **128**, 407.

Kafka, F. Y. & Dussan V., E. B. 1979 On the interpretation of dynamic contact angles in capillaries. *J. Fluid Mech.* **95**, 539.

Kistler, S. F. 1993 Hydrodynamics of wetting. In *Wettability* (ed. J. C. Berg). M. Dekker.

Koplik, J., Banavar, J. R. & Willemsen, J. F. 1988 Molecular dynamics of Poiseuille flow and moving contact lines. *Phys. Rev. Lett.* **60**, 1282.

Langmuir, I. 1920 The mechanism of the surface phenomena of flotation. *Trans. Faraday Soc.* **15**, 62.

Langmuir, I. 1938 Overturning and anchoring of monolayers. *Science* **87**, 493.

Marsh, J. A., Garoff, S. & Dussan V., E. B. 1993 Dynamic contact angles and hydrodynamics near a moving contact line. *Phys. Rev. Lett.* **70**, 2778.

Ngan, C. G. & Dussan V., E. B. 1989 On the dynamics of liquid spreading on solid surfaces. *J. Fluid Mech.* **209**, 191.

† This author's name was misspelled as Hadjicostantinou in the original reference.

Petrov, J. G. 1986 Dependence of the maximum speed of wetting on the interactions in the three-phase contact zone. *Colloids and Surfaces* **17**, 283.

Petrov, J. G., Kuhn, H. & Möbius, D. 1980 Three-phase contact line motion in the deposition of spread monolayers. *J. Colloid Interface Sci.* **73**, 66.

Petrov, J. G. & Sedev, R. V. 1985 On the existence of a maximum speed of wetting. *Colloids and Surfaces*, **13**, 313.

Ramé, E. 1988 On the spreading of liquids in the presence of surfactants. PhD Thesis, University of Pennsylvania, Philadelphia, USA.

Rosenblat, S. & Davis, S. H. 1985 *Frontiers in Fluid Mechanics. A Collection of Papers Written in Commemoration of the 65th Birthday of Stanley Corrsin* (ed. S. H. Davis & J. L. Lumley), pp. 171. Springer.

Sedev, R. V. & Petrov, J. G. 1991 The critical condition for transition from a steady wetting to film entrainment. *Colloids and Surfaces* **53**, 147.

Sheng, P. & Zhou, M. 1992 Immiscible fluid displacement: contact line dynamics and the velocity-dependent capillary pressure. *Phys. Rev.* A **45**, 5694.

Shikhmurzaev, Y. D. 1993 The moving contact line on a smooth solid surface. *Intl J. Multiphase Flow* **19**, 589.

Shikhmurzaev, Y. D. 1997 Moving contact lines in liquid/liquid/solid systems. *J. Fluid Mech.* **334**, 211.

Thompson, P. A. & Robbins, M. O. 1989 Simulation of contact line motion: slip and the dynamic contact angle. *Phys. Rev. Lett.* **63**, 766.

Thompson, P. A. & Troian, S. M. 1997 A general boundary condition for liquid flow at solid surfaces. *Nature* **389**, 360.

Troian, S. M., Herbolzheimer, E. & Safran, S. A. 1990 Model for the fingering instability of spreading surfactant drops. *Phys. Rev. Lett.* **65**, 333.

Voinov, O. V. 1994 Closure of the hydrodynamic theory of wetting in a small-scale region. *J. Appl. Mech. Tech. Phys.* **35**, 1.

Weidner, D. E. & Schwartz, L. W. 1994 Contact-line motion of shear-thinning liquids. *Phys. Fluids* **6**, 3535.